UNIVERSIDAD NACIONAL AUTÓNOMA DE MÉXICO
POSGRADO EN CIENCIAS FÍSICAS
INSTITUTO DE FÍSICA

Universal intermediate phase of bulk eigenvalues in the Ginibre ensemble

TESIS
Que para optar por el título de:
Maestro en ciencias (Física)

PRESENTA:
Jeyson Andrés Monroy Garzón

TUTOR PRINCIPAL:
Dr. Isaac Pérez Castillo
Instituto de Física, UNAM

COMITÉ TUTOR:
Dr. Gerardo Ruiz Chavarría
Facultad de Ciencias, UNAM
Dr. José David Vergara Oliver
Instituto de Ciencias Nucleares, UNAM

Ciudad de México, México, Septiembre de 2019

Dedicated to my family who have always supported me in my life and my personal projects

Thermodynamics, correctly interpreted, does not just allow Darwinian evolution; it favors it.

Ludwig Boltzmann

Abstract

The main goal of this MSc thesis is to present a complete theory for the full order statistics of the complex Ginibre ensemble of $N \times N$ random matrices. This consists of an ensemble of matrices whose complex entries are independently drawn from a Gaussian distribution and, unlike the classical random matrix ensembles, no other symmetries are imposed on it. One can show that this system is mathematically equivalent to a two dimensional gas of charged particles with inter-particle logarithmic repulsion in the presence of a convex harmonic potential. We study the statistical properties of the number particles inside a circle of radius r, the so-called index number, which is equivalent to the order statistics for the radial position of each particle. We are able to derive exact formulas describing the fluctuations of the index number for typical and large fluctuations. Moreover, we show that, as in the case for the statistics of the extremal particle, there exists an intermediate fluctuation regime that interpolates smoothly between the large and the typical fluctuations. Our analytical results are successfully compared with reweighted Monte Carlo simulations.

This thesis is structured as follows: we first give a brief overview on large deviation theory, providing a simple example, that of a coin tossing, encapsulating the main ideas. We then move on to provide the basic definitions and results of random matrix theory. We devote the rest of the thesis to present the aforementioned results.

The results presented in this MSc thesis (which were carried out together with Bertrand Lacroix-A-Chez-Toine, Isaac Pérez Castillo, Anupam Kundu, Satya N. Majumdar, Grégory Schehr and Christopher Sebastian Hidalgo Calva) have been recently published in the article entitled: *"Intermediate deviation regime for the full eigenvalue statistics in the complex Ginibre ensemble"*, Physical Review E 100 (1), 012137 (2019).

Resumen

El objetivo principal de este trabajo es presentar una teoría completa sobre *la estadística de orden completo* en el ensamble complejo de matrices de Ginibre de tamaño $N \times N$. Este ensamble consiste en matrices cuyas entradas son independientes, obtenidas a partir de una distribución Gaussiana y, a diferencia de los ensambles de matrices aleatorias clásicos, este no presenta ninguna simetría. Uno puede demostrar que este sistema es matemáticamente equivalente a un gas de partículas cargadas dos-dimensional que se repelen mediante un potencial logarítmico en presencia de un potencial armónico externo. Estudiamos las propiedades estadísticas del número de eigenvalores dentro de un círculo de radio r, las cuales son equivalentes al orden estadístico de la posición radial de cada partícula. En este trabajo derivamos fórmulas exactas para describir las fluctuaciones del número de eigenvalores en el regimen de fluctuaciones típico y atípico. Además, mostramos que, de forma análoga al caso de la estadística de valores extremos, existe un regimen de fluctuaciones intermedio que es capaz de conectar suavemente los regímenes de fluctuaciones típicas y atípicas. Los resultados son comparados exitosamente con simulaciones Monte Carlo.

Esta tesis esta estructurada como sigue: primero damos una breve descripción general sobre teoría de grandes desviaciones, donde proveemos un ejemplo simple sobre el lanzamiento de N monedas, el cual encapsula las ideas principales. Luego damos conceptos y resultados importantes en teoría de matrices aleatorias. En el resto de este trabajo presentamos los resultados mencionados.

Los resultados presentados en esta tesis de maestría (que fueron llevados a cabo en cojunto con Bertrand Lacroix-A-Chez-Toine, Isaac Pérez Castillo, Anupam Kundu, Satya N. Majumdar, Grégory Schehr y Christopher Sebastian Hidalgo Calva) han sido publicados en un artículo titulado *Intermediate deviation regime for the full eigenvalue statistics in the complex Ginibre ensemble*, Physical Review E 100 (1), 012137 (2019).

Contents

List of figures VII

1. Large deviation theory 2
1.1. Large deviation principle . . . 3
1.2. A simple example: coin tossing . . . 4

2. Random matrix theory 7
2.1. Introduction to random matrix theory . . . 7
2.2. Gaussian ensembles . . . 7
2.3. Ginibre ensembles . . . 9

3. Intermediate deviation regime for the full eigenvalue statistics in the complex Ginibre ensemble 13
3.1. Exact results for finite N . . . 14
3.2. The limit of large N . . . 15
3.2.1. Regime of typical fluctuations . . . 16
3.2.2. Regime of intermediate fluctuations . . . 17
3.2.3. Regime of atypical fluctuations . . . 19

4. Comparison with Monte Carlo simulations 21

5. Conclusions and outlook 24

A. Derivation of exact results for finite N 25
A.1. Exact probability of having $N_r = K$ eigenvalues . . . 25
A.2. Cumulants for finite N . . . 26

B. Useful results for large N 28
B.1. Inverse Laplace integral . . . 28
B.2. Asymptotic behavior of $L_{xN}(r)$ and $M_{xN}(r)$ . . . 28
B.3. Derivation of the mean and variance of κ . . . 31
B.3.1. Expected value of κ in the Ginibre ensemble . . . 31
B.3.2. Variance of κ in the Ginibre ensemble . . . 31

C. Intermediate deviation regime 33
C.1. Asymptotic behaviour of the scaling function $\chi(\mu)$ for small μ . . . 33
C.2. Asymptotic behaviour of the scaling function $\chi(\mu)$ for large $|\mu|$ . . . 33

D. Saddle point equation for the atypical regime **35**

Bibliography **36**

List of figures

1-1. Plot of $\log P(M,N)$ given by the formula (1-5) (square symbols), the Gaussian approximation given by central limit theorem in the equation (1-6) (solid blue line) and the approximation given by large deviation theory given by eq. (1-8) (solid red line) for $N = 1000$. 5

2-1. Density of eigenvalues in Gaussian ensembles which is described by Wigner semicircular law for large matriz size. The above distribution was obtained by Monte Carlo simulation for a matrix size of $N = 500$ averaging over 1000 samples. 9

2-2. Distribution of eigenvalues in the complex plane for a Ginibre ensemble for a spherical potential $V(z) = v(|z|) = r^2$. This distribution was obtained by Monte Carlo simulations for $N = 1000$ eigenvalues. 10

3-1. In this figure we show a number of K eigenvalues for a Ginibre ensemble inside a disk of radius r (red curve). The previous was obtained for a matrix of size $N = 1000$. 13

4-1. In this figure is compared the theoretical first four cumulants of N_r as a function of r (solid blue line) with Monte Carlo simulations (red dots). The simulations were performed for $N = 100$ and averaging over $1{,}2 \times 10^7$ samples 21

4-2. This figure shows the numerical results of $-\frac{1}{N}\log \mathcal{P}_r(\kappa, N)$ obtained by "importance" sampling tecniques (blue circular markers) and the theoretical results for typical (solid black curve), intermediate (solid green curve) and atypical (solid red curve) fluctuations of κ for $N = 500$ eigenvalues and $r = 1/2$. The simulations were performed for a set of values of β between -333 and 117 in steps of 4.5 and using 2.8×10^5 samples. 23

B-1. In this figure we can see the Bromwich contour $\mathcal{C}$, given by the solid black line, and the singularities of $f(s)$ which are to the left of $\mathcal{C}$. 28

1. Large deviation theory

Events such as earthquakes, overflows or river droughts, or financial crises are events that do not happen daily. However, when they do occur, they have, more often than not, catastrophic consequences [1]. Then, it is desirable to have a mathematical tool that accurately models the probabilities of occurrences of these rare events. To provide a little intuition, consider the behavior of the height of the water level of a river and suppose we save the data to obtain an empirical histogram, i.e. its probability distribution. From this histogram, fluctuations around the expected value can be well-approximated by a Gaussian distribution justified by the central limit theorem (CLT). But if we were interested in obtaining exactly the probability of rare events, which are important to describe cases of droughts or overflows, the CLT is unable to capture properly the probability of such events [1]. Thus, we need a complete theory that enables us to explore the statistics of these extreme events. This approach is called large deviation theory.

The first formulation of this theory was introduced in 1930s by Cramér to describe the probability of the sample mean $y_N = (x_1 + x_2 + \cdots + x_N)/N$ for a set of N independent and identically distributed random variables x_i. This theory is especially useful to deal with those events which result in a value of y_N far away from its mean $\langle y_N \rangle$, and captures how the probability of such events decays exponentially fast as N increases [2, 3]. This approach can generally be thought as a generalization of the central limit theorem for independent or weakly correlated random variables since, as we will exemplify below, it is also able to accurately deal with those events that yield a value of y_N close to its mean [4].

Physicists may not be aware about the theory of large deviations, but it appears naturally in the area of condensed matter physics and statistical mechanics, when one is trying to determine the equilibrium properties of many-particle systems. The first encounter to the formal idea of large deviations is through the use of the techniques such as Laplace's or saddle-point methods. You could even say that, in the same manner differential geometry is the mathematical language of general relativity, large deviation theory is the natural mathematical language of statistical physics. Actually, one of the most relevant results of the large deviation theory is the generalization of Einstein's fluctuation theory which states that probabilities can be expressed in terms of entropy functions. Large deviation theory explains too why free energies and entropy are related by a Legendre transformation in thermodynamics. It also explains why the state of a system in equilibrium can be determined from extreme principles, such as maximum entropy and minimal energy [3].

It is not the main goal of this thesis to provide formal definitions about large deviation theory, nonetheless, we feel obliged to present the large deviation principle (LDP) in a mathematical ligther framework, familiar to seasoned physicists.

1.1. Large deviation principle

Large deviation theory simply states that the probability that the random variable y_N is smaller than a value y behaves asymptotically for large N in the following form [2, 5]:

$$P_N(y) = \text{Prob}[y_N \leq y] \asymp \begin{cases} e^{-w_N^{(-)}\psi^{(-)}(y)} & , \quad y < \langle y_N \rangle \\ 1 - e^{-w_N^{(+)}\psi^{(+)}(y)} & , \quad y > \langle y_N \rangle \end{cases} , \tag{1-1}$$

where $\psi^{(-)}(y)$ and $\psi^{(+)}(y)$ are the so-called rate functions that control the probability that y_N takes values smaller or larger than $\langle y_N \rangle$, respectively. Here, the terms $w_N^{(-)}$ and $w_N^{(+)}$ characterise the decaying speed, which in general depends on N. Being more precise, by asymptotic behavior (denoted with the symbol $\asymp$ in the expression above) we mean that $P_N(y)$ satisfies a *large deviation principle* if the following limits exist

$$-\lim_{N\to\infty} \frac{1}{w_N^{(-)}} \log P_N(y) = \psi^{(-)}(y) \tag{1-2}$$

$$-\lim_{N\to\infty} \frac{1}{w_N^{(+)}} \log(1 - P_N(y)) = \psi^{(+)}(y), \tag{1-3}$$

and they are different from zero. To ensure this, the terms $w_N^{(+)}$ and $w_N^{(-)}$ must be chosen so as to obtain nontrivial results [2, 3]. Intuitively, this limit tells us that the dominant behavior of $P_N(y)$ is a decaying exponential in $w_N^{(\pm)}$ for large N [3]. It is worthwhile mentioning that, if the above limit is zero, we say that $P_N(y)$ decays sub-exponentially in $w_N^{(\pm)}$, or if the limit diverges, we say that the probability, $P_N(y)$, decays super-exponentially [3]. One can also show that this result implies that the probability density function (PDF) of y_N has the following behavior [4]

$$\text{Prob}(y_N = y) \asymp e^{-W_N \Psi(y)}, \qquad W_N\Psi(y) = \begin{cases} w_N^{(-)}\psi^{-}(y) & , \quad y < \langle y_N \rangle \\ w_N^{(+)}\psi^{+}(y) & , \quad y > \langle y_N \rangle \end{cases} \tag{1-4}$$

or, in other words, we say that $p_N(y)$ satisfies a large deviation principle with speed rate W_N and rate function $\Psi(y)$ [3, 2, 5].

Let us enumerate some properties of the rate function $\Psi(y)$ for the simplest case of the empirical mean, $y_N = \frac{1}{N}\sum_{i=1}^{N} x_i$, where x_i are independent and identically distributed or weakly correlated. In this situation, the rate function $\Psi(y)$, also called Cramér function, is a convex function, i.e. $\Psi''(y) > 0$, which satisfies the following properties

- $\Psi(y) = 0$ for $y = \langle y_N \rangle$
- $\Psi(y) > 0$ for $y \neq \langle y_N \rangle$
- $\Psi(y) \approx (y - \langle y_N \rangle)^2 / 2\sigma^2$, with variance $\sigma^2 = \frac{1}{\Psi''(y)}\Big|_{y=\langle y_N \rangle}$, for y near $\langle y_N \rangle$.

Note that the third property corresponds to the central limit theorem (CLT), which states that fluctuations of y_N around its expected value are Gaussian distributed for independent or weakly

correlated random variables [4, 6]. Thus, the large deviation theory can be thought of as a generalization of CLT.

The interested reader can find a more formal treatment of the large deviation principle in [3, 7, 8, 9, 10].

1.2. A simple example: coin tossing

Suppose we have N unbiased coins and we toss them at the same time. Let N_h denote the number of heads. If we repeat this experiment a certain number of times and record the value of N_h, its value will fluctuate between 0 and N, as this is clearly a stochastic process. Thus, the probability of the event $N_h = M$, denoted by $P(M, N) = \text{Prob}(N_h = M)$, is the binomial distribution [6]

$$P(M, N) = \frac{1}{2^N} \binom{N}{M} . \tag{1-5}$$

If we plot $P(M, N)$ as a function of M and for $N = 1000$, we have that for values of M near the mean ($\langle M \rangle = 500$), this distribution has a bell-shaped form with mean and variance given by $N/2$ and $\sigma^2 = N/4$, respectively. By using the CLT, we can approximate the typical fluctuations of N_h by the following Gaussian distribution [1]

$$P(M, N) \approx \sqrt{\frac{2}{N\pi}} e^{-\frac{2}{N}(M-N/2)^2} . \tag{1-6}$$

The comparison between the exact expression $P(M, N)$ and that obtained by the Gaussian approximation is shown in figure **1-1**. From this, we can see that the Gaussian approximation (blue solid line) fails to describe the correct distribution (square black symbols) away from the mean value, as we expected by the CLT. To illustrate this discrepancy, consider the particular case of all the coins giving head. The probability of this event, $N_h = N$, is

$$P(M = N, N) = \text{Prob}(N_h = N) = \frac{1}{2^N} = e^{-N \ln(2)} , \tag{1-7}$$

while if we were to naively use $M = N$ in the Gaussian approximation, we would obtain $P(N, N) \approx e^{-N/2}$. Thus, the latter result is bigger than the exact probability, failing to quantify correctly the probability of a rare event.

One may have intuitively noticed that rare events are those for which fluctuations of N_h are of order N rather than $\sqrt{N}$. With this in mind, let us set $M = cN$ with $c \in [0, 1]$ in the equation (1-5), so that we can write

$$\text{P}(M = cN, N) = \frac{1}{2^N} \frac{N!}{(cN)![(1-c)N]!} . \tag{1-8}$$

Next, using Stirling's approximation [11] for large N we obtain that the probability distribution $P(M, N)$ becomes

$$\text{P}(M = cN, N) \asymp e^{-N\phi(c)}, \quad \phi(c) = c \ln(c) + (1-c) \ln(1-c) + \ln(2) . \tag{1-9}$$

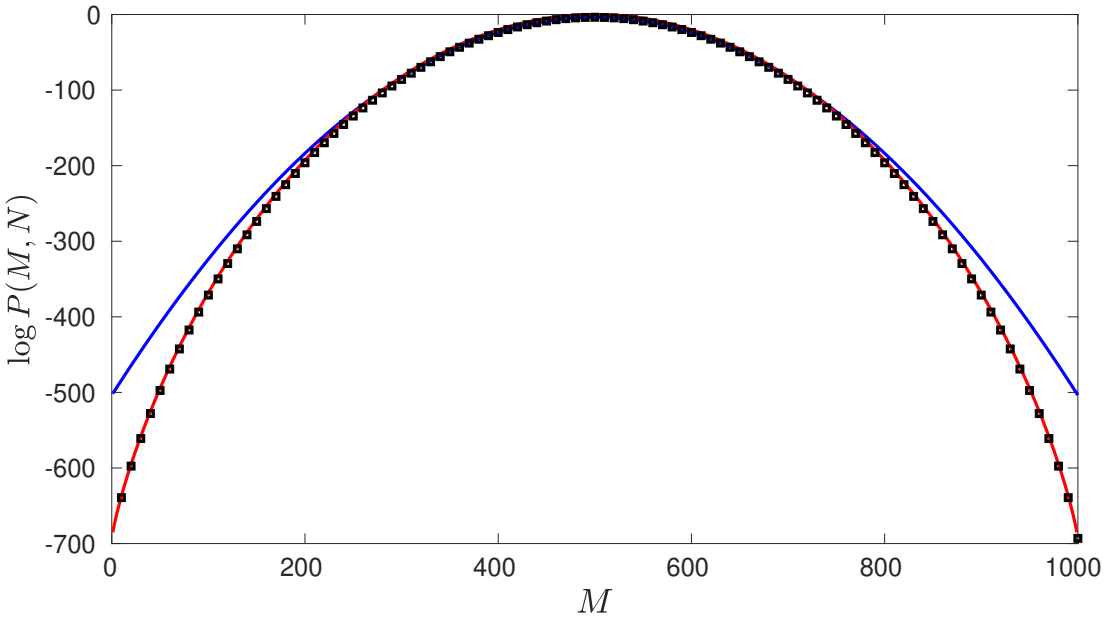

Figure **1-1**.: Plot of $\log P(M,N)$ given by the formula (1-5) (square symbols), the Gaussian approximation given by central limit theorem in the equation (1-6) (solid blue line) and the approximation given by large deviation theory given by eq. (1-8) (solid red line) for $N = 1000$.

This is our first simple example of a large deviation principle. It says that the probability of the event $N_h = cN$ decays exponentially fast with speed N and rate function $\phi(c)$ [1]. This rate function has the following main properties: i) it is a convex function; ii) its minimum is located at $c = 1/2$, precisely the typical value of N_h/N. Moreover, when evaluated at $c = 1$, which corresponds to the event $N_h = N$, we obtain that $\phi(c = 1) = \ln(2)$, recovering the exact result. Additionally, if we expand $\phi(c)$ around its minimum, we obtain $\phi(c) \approx 2(c-1/2)^2$, which, after substituting $c = M/N$, yields back the Gaussian approximation given by eq. (1-6). Thus, we have that CLT is captured by the large deviation theory. The behaviour of the result obtained by the large deviation theory are also shown in the figure **1-1** (solid red line).

Physicists may be inadvertently aware of the concepts of large deviation theory, perhaps presented in a different language. To put it in context, consider the same problem of coin tossing, but instead of asking about the probability of obtaining the number of heads, let us consider the number of possible configurations that will give M heads [1]. This is given by

$$\mathcal{N}(M) = \binom{N}{M}. \tag{1-10}$$

Taking again $M = cN$, and for large N, we obtain

$$\mathcal{N}(M) \asymp e^{NS(c=\frac{M}{N})}, \tag{1-11}$$

where $S(c)$ reads

$$S(c) = \ln(2) - \phi(c) = -c\ln(c) - (1-c)\ln(1-c)\,. \tag{1-12}$$

Thus, mathematicians will say that the number of configurations given by eq. (1-10) admits a large deviation principle with rate function $S(c)$. For physicists, on the other side, the rate function $S(c)$ is nothing but the entropy density. This can be made a bit more precise by noting that the experiment of coin tossing corresponds to that of N non-interacting Ising spins $s_i \in \{-1, +1\}$ subjected to an external magnetic field h. The energy configuration of this system is $E = -h\sum_{i=1}^{N} s_i$. If we particularize to $h = -1/2$ and do a change of variables $s_i = 2\sigma_i - 1$, with $\sigma_i \in \{0, 1\}$, then we have that

$$E = \sum_{i=1}^{N} \sigma_i\,, \tag{1-13}$$

so the energy E coincides with the number of heads, N_h. In this context, the number of spin configurations for a fixed value of energy, $\mathcal{N}(E)$, is known as the *micro-canonical* partition function. The corresponding entropy per spin $S(c = E/N)$ is thus given by the same formula as the coin tossing problem. This, of course, in the context of statistical physics, also applies for any external field h.

Similarly, we can find a large deviation principle in the canonical ensemble. To realize this, we start from the following integral

$$Z = \int e^{-\beta E}\mathcal{N}(E)dE\,, \tag{1-14}$$

known as the canonical partition function. To solve this integral, we use that in the limit of large N, we have that $\mathcal{N}(E) \asymp e^{NS(c=E/N)}$, and therefore

$$Z = N\int dc e^{-\beta N[c - S(c)/\beta]}\,. \tag{1-15}$$

The above equation for large N can be solved by the saddle-point method, yielding

$$Z = e^{-\beta N \min_c[c - S(c)/\beta]}. \tag{1-16}$$

Since, in the thermodynamic limit, the free energy per particle is given by $f(\beta) = -\lim_{N\to\infty}\frac{1}{\beta N}\ln Z$, we conclude that the canonical partition function Z follows a large deviation principle with velocity N and rate function given by the free energy $\beta f(\beta)$. Note that the entropy in the microcanonical ensemble and the free energy in the canonical ensemble are related by a Legendre transformation.

Up to this point, we have discussed the case of N independent random variables in both a mathematical and a physical setting. For correlated random variables (interacting physical systems) we expect phase transitions to occur, which reveal themselves as non-analyticities on the rate functions (free energies).

2. Random matrix theory

2.1. Introduction to random matrix theory

The theory of random matrices originated in the 1920s and the 1950s with the seminal works of Wishart and Wigner in the areas of random covariance matrices and heavy nuclei, respectively. Since then, this area of research has gained great popularity due to the variety of applications ranging from combinatorics [12], stochastic growth [13] financial data [14], the metric of a manifold [15] or the statistics of extreme value (EVS) for strongly correlated random variables [16].

Generally speaking, ensembles of random matrices offer the perfect mathematical laboratory to study a system of strongly correlated random variables: that of its eigenvalues. As we want to understand how the universal laws concerning, for instance, EVS for independent and identically distributed random variables do change for strongly correlated systems, we will solely focus in the use of random matrix theory in this subtopic of statistics and probability. For applications of random matrix theory in other areas, we point the reader to the standard literature on the field and a variety of review articles already in existence.

In this chapter, we briefly introduce the Gaussian and Ginibre ensembles, and discuss their use in exploring the concepts of extreme value statistics and full counting statistics.

2.2. Gaussian ensembles

The Gaussian matrix ensembles were introduced by Wigner and mathematical formalized by Dyson. The original goal was to approximate Hamiltonian systems describing heavy nuclei by considering a random matrix representation of them and keeping only their most basic ingredients: symmetries. This gave back three random matrix ensembles: the Gaussian Orthogonal Ensemble (GOE), the Gaussian Unitary Ensemble (GUE), and the Gaussian Symplectic Ensemble (GSE). As the matrices are random, so are their eigenvalues and it turns out that for the Gaussian ensembles it is possible to derive exactly the joint distribution of eigenvalues. Indeed, if we consider matrices of size $N \times N$ and denote the eigenvalues as $(\lambda_1, \lambda_2, ...\lambda_N)$, then the joint distribution of eigenvalues is given by [17]:

$$P_{\text{joint}}(\lambda_1, \lambda_2, ..., \lambda_N) = \frac{1}{Z_{N,\beta}} \prod_{i<j} |\lambda_i - \lambda_j|^\beta \prod_{k=1}^{N} e^{-\frac{\beta}{2}\lambda_k^2}, \tag{2-1}$$

where $Z_{N,\beta}$ is the normalization factor, and $\beta \in \{1, 2, 4\}$ is known as the Dyson index, whose value is related to a particular ensemble: $\beta = 1$ for GOE, $\beta = 2$ for GUE, and $\beta = 4$ for the GSE ensemble. Notice that the term $\prod_{i<j} |\lambda_i - \lambda_j|^\beta$ in the joint distribution of eigenvalues makes them

to be a strongly correlated system in which the eigenvalues repel each other.

Notice that $P_{\text{joint}}(\lambda_1, \lambda_2, ..., \lambda_N)$ can be re-interpreted in the context of statistical physics if we rewrite it as the Gibbs-Boltzmann distribution $P_{\text{joint}}(\lambda_1, \lambda_2, ..., \lambda_N) = \frac{e^{-\beta E(\{\lambda_i\})/2}}{Z_{N,\beta}}$ with

$$E(\{\lambda_i\}) = \sum_{k=1}^{N} \lambda_k^2 - \sum_{i \neq j} \log|\lambda_i - \lambda_j| \,. \tag{2-2}$$

This so-called Dyson's log-gas can be interpreted as a two-dimensional interacting gas of charged particles constrained to a one-dimensional line and with an external harmonic potential. While Dyson's index β plays the role of inverse temperature, within this interpretation, β could well be any positive real value. Interestingly, there actually exists a matrix representation for such cases, given in terms of tridiagonal random matrices [18, 19, 20].
Expressions of the sort (2-1) are very appealing mathematically, as they allow to study many statistical properties of strongly correlated variables exactly. Indeed, let us start by considering a simple statistics: the average density of eigenvalues. This is given by:

$$\rho_N(\lambda) = \left\langle \frac{1}{N} \sum_{i=1}^{N} \delta(\lambda - \lambda_i) \right\rangle, \tag{2-3}$$

where $\langle \cdots \rangle$ is an average with respect to the joint PDF given in equation (2-1). It can be shown that, if we rescale $\lambda \to \sqrt{N}\lambda$ and take the limit when $N \to \infty$, we obtain the celebrated *Wigner semi-circular law* [17]:

$$\lim_{N\to\infty} \rho_N(\lambda) = \tilde{\rho}_{sc}(\lambda) = \frac{1}{\pi}\sqrt{2 - \lambda^2}, \tag{2-4}$$

which has a support $[-\sqrt{2}, \sqrt{2}]$. A plot of this limiting density can be seen in figure **2-1**. Notice that in the limit of large N we obtain that the mean value of the maximum eigenvalue is $\sqrt{2}$. One can study the statistics of the maximum eigenvalue for finite N to probe how EVS changes for strongly correlated random variables [19]. This can done using various mathematical techniques. For instance, if we define the cumulative distribution function (CDF) for the largest eigenvalue $\lambda_{\max}$ as

$$F_N(w) = \text{Prob}[\lambda_{\max} \leq w], \tag{2-5}$$

this can be recast as a ratio of two partitions functions as

$$F_N(w) = \frac{Z_N(w)}{Z_N(w \to \infty)} \,, \tag{2-6}$$

with

$$Z_N(w) = \int_{-\infty}^{w} d\lambda_1 \cdots \int_{-\infty}^{w} d\lambda_N \exp\left[\frac{\beta}{2}\left(N\sum_{i=1}^{N}\lambda_i^2 - \sum_{i\neq j}\ln|\lambda_i - \lambda_j|\right)\right]. \tag{2-7}$$

Being brief with the findings in [19], after appropriately rescaling $F_N(w)$, the limiting CDF for the maximum eigenvalue follows a new universal law, departing from the iid case of EVS given by the Tippett-Fisher-Gnedenko theorem [21, 22] . This new law is the celebrated Tracy-Widom

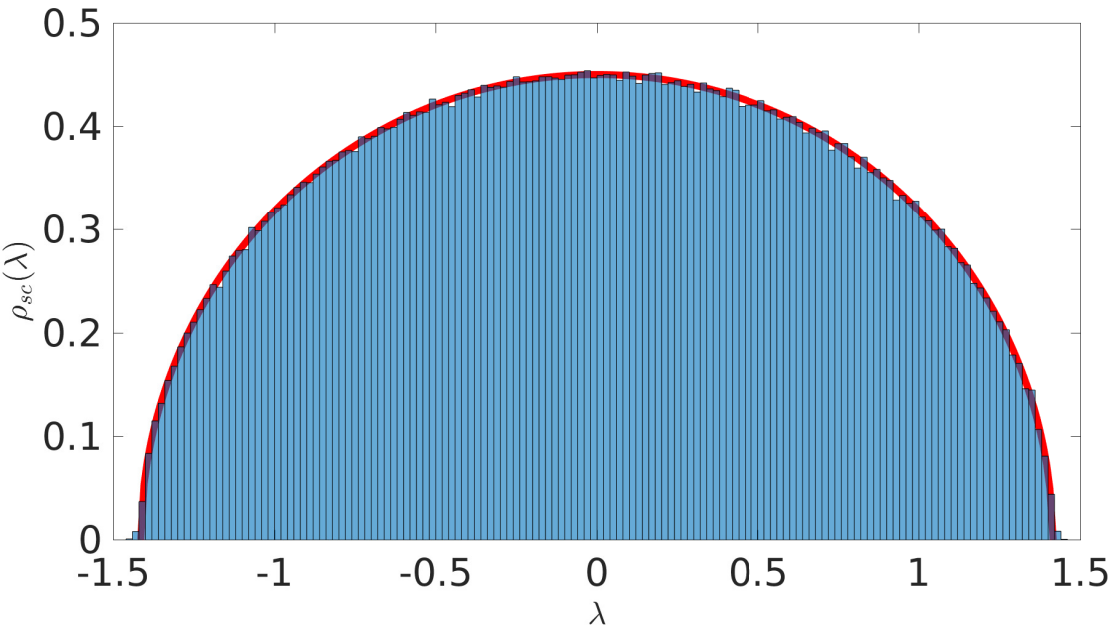

Figure **2-1**.: Density of eigenvalues in Gaussian ensembles which is described by Wigner semicircular law for large matriz size. The above distribution was obtained by Monte Carlo simulation for a matrix size of $N = 500$ averaging over 1000 samples.

distribution [23] .

The findings about statistical properties of extreme eigenvalues can also be generalised to bulk eigenvalues by introducing the so-called *full counting statistics* (FCS) of the *index number* $\mathcal{N}_{\mathcal{D}}$, which counts how many eigenvalues are in a given domain $\mathcal{D}$. For instance, the probability of having exactly K eigenvalues, $\text{Prob}(\mathcal{N}_{\mathcal{D}} = K) = P_{\mathcal{D}}(K, N)$, in the domain $\mathcal{D} = \{L \in \mathbb{R}, 0 < L < \sqrt{2}\}$ (bulk) has a Gaussian behavior in the typical regime [24, 25, 26, 27], while the large fluctuations [28, 29] of $\mathcal{N}_{\mathcal{D}}$ follows the large deviation principle $P_{\mathcal{D}}(K, N) \asymp e^{-N^2\psi_L(K/N)}$, where $\psi_L(K/N)$ behaves quadratic around its minimum and match smoothly with the typical regime. This motivates the general purpose of this thesis, in which we will consider the full counting statistics of the number $\mathcal{N}_{\mathcal{D}}$ in the Ginibre ensemble.

2.3. Ginibre ensembles

Another kind of random matrices are the complex Ginibre ensemble which was proposed by Jean Ginibre in 1964 [30, 17]. The entries of those matrices of size $N \times N$ are composed by random complex numbers where the real and imaginary parts follow a Gaussian distribution with zero mean and variance $\mathcal{O}(1/N)$. Consequently, the eigenvalues are random complex variables, which are

distributed in the complex plane according to the following joint probability distribution function

$$P_{\text{joint}}(z_1, ..., z_N) = \frac{1}{Z_N} \prod_{i<j} |z_i - z_j|^2 \prod_{k=1}^{N} e^{-NV(z_k)}, \tag{2-8}$$

where the constant Z_N is a normalization factor, and $V(z) = |z|^2$. From the physics point of view, the equation (2-8) can be understood as a Gibbs-Boltzmann distribution associated with a 2-d Coulomb gas of N particles, where each particle is subjected to an harmonical external confining potential and are repealing each other via the 2-d Coulomb logarithmic repulsive potential. Interestingly, the joint (PDF) can be mapped onto the ground-state wave function of N non-interacting fermions on a plane in the presence of a perpendicular magnetic field [16].
As in the Gaussian ensemble, expression in eq.(2-8) offers us the possibility to study some statistical properties of the eigenvalues. For instance, the average density in eq. (2-3) converges in the limit when $N \to \infty$ to the so-called Girko's circular law given by (see figure **2-2**)

$$\lim_{N\to\infty} \rho_N(z) = \pi^{-1}\Theta(r_{\text{edge}} - |z|), \tag{2-9}$$

where $\Theta(x)$ is the heaviside step function and $r_{\text{edge}} = 1$.

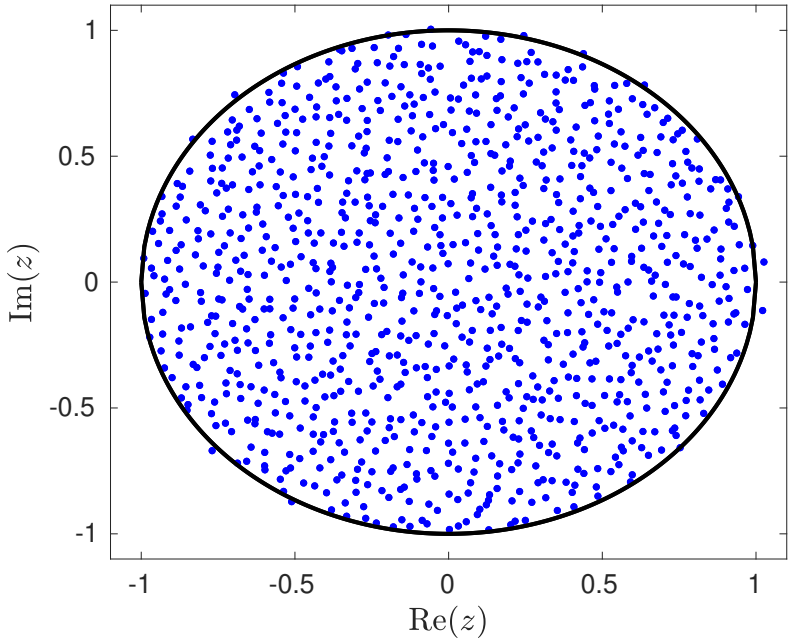

Figure **2-2**.: Distribution of eigenvalues in the complex plane for a Ginibre ensemble for a spherical potential $V(z) = v(|z|) = r^2$. This distribution was obtained by Monte Carlo simulations for $N = 1000$ eigenvalues.

Moreover, for a large but finite N, it can be shown that the density of eigenvalues has the form

$$\rho_N(z) = \rho_b(r_{\text{edge}})\tilde{\rho}\left(\frac{r - r_{\text{edge}}}{\Delta_N}\right), \qquad \tilde{\rho}(x) = \frac{1}{2}\text{erfc}(x)\,, \tag{2-10}$$

where $\Delta N = (2N)^{-1/2}$, $\mathrm{erfc}(x)$ is the complementary error function and $\rho_b(r_{\mathrm{edge}}) = \pi^{-1}$ [16]. Note that in the asymptotic limit when $x \to -\infty$, $\mathrm{erfc}(x) \sim 1$ and we recover Girko's circular law for bulk elements (for $r < r_{\mathrm{edge}}$) while for $x \to \infty$, $\mathrm{erfc}(x) \sim e^{-x^2}/(2\sqrt{\pi}x)$ and we obtain that the eigenvalues density vanishes exponentially fast far from the edge [16, 31, 32].

Moreover, interesting properties can be derived for the random variable $r_{\max} = \max_{1\leq i\leq N}\{|z_i|\}$ such as the Cumulative Distribution Function (CDF) with the form

$$Q_N(w) = \mathrm{Prob}(r_{\max} \leq w) = \prod_{k=1}^{N} q_k(w), \qquad q_k(w) = \frac{\int_0^w r^{2k-1}e^{-Nv(r)}dr}{\int_0^\infty r^{2k-1}e^{-Nv(r)}dr}, \tag{2-11}$$

with $v(r)$ an arbitrary spherical potential. Equation (2-11) tells us that $r_{\max}$ is the maximum among a collection of independent random variables x_k drawn from a different probability distribution $q_k(w) = \mathrm{Prob}[x_k \leq w]$. From equation (2-11) one can derive the CDF in the limit of large N and find that there are three different kind of fluctuations around the mean value with different scales which are summarized as follows (see ref. [16])

$$Q_N(w) \sim \begin{cases} e^{-N^2\Phi_-(w)+o(N^2)} & \text{for} \quad 0 < r_{\mathrm{edge}} - w = \mathcal{O}(1) \\ e^{-\frac{r_{\mathrm{edge}}}{\Delta_N}\Phi_I\left(\frac{w-r_{\mathrm{edge}}}{\Delta_N}\right)} & \text{for} \quad 0 < r_{\mathrm{edge}} - w = \mathcal{O}(\Delta_N) \\ G(a_N(w-b_N)) & \text{for} \quad w - b_N = \mathcal{O}(a_N^{-1}) \\ 1 - e^{-N\Phi_+(w)+o(N)} & \text{for} \quad w - b_N = \mathcal{O}(1) \end{cases}. \tag{2-12}$$

In the third line of the above equation we read that the typical fluctuations of $r_{\max}$ are $\mathcal{O}(1/a_N)$ and obeys a Gumbel law with $G(x) = e^{-e^{-x}}$ where the scaling factors a_N and b_N have the form

$$a_N = \sqrt{4NC_N}, \quad b_N = 1 + \sqrt{\frac{C_N}{4N}}, \quad C_N = \ln N - 2\ln\ln N - \ln 2\pi. \tag{2-13}$$

In the the first and fourth lines we have that the regimes of large fluctuations with $r_{\mathrm{edge}} - w \sim \mathcal{O}(1)$, follows a large deviation principle for the left and right tail with rate functions given by (for more details see [33])

$$\begin{aligned} \Phi_-(w) &= \frac{1}{4}(4w^2 - w^4 - 4\ln w - 3), \quad \text{for} \quad 0 < w < 1 \\ \Phi_+(w) &= w^2 - 2\ln w - 1 \quad \text{for} \quad w > 1 \end{aligned}. \tag{2-14}$$

Finally, in the second line an intermediate regime is introduced as a consequence of a mismatch between the large left fluctuations and the central regime. This intermediate phase can be modeled by a new rate function $\Phi_I(y)$ which interpolates smoothly the left tail with the central distribution and have the asymptotic limit (see ref. [16] for more details)

$$\Phi_I(y) \sim \begin{cases} \frac{|y|^3}{3} + |y|\ln|y| + \mathcal{O}(y) & y \to -\infty \\ \frac{e^{-y^2}}{2\sqrt{\pi}y^2} & y \to +\infty\,. \end{cases} \tag{2-15}$$

The behavior for the large fluctuations for the bulk elements was already computed in [34] when $N \to \infty$ finding that the PDF $\mathcal{P}_r(\kappa, N)$ that the fraction κ of eigenvalues inside the domain

$\mathcal{D} = \{z : z \in \mathbb{C}, |z| \leq r\}$, follows a large deviation principle $\mathcal{P}_r(\kappa, N) \asymp e^{-N^2\psi_r(\kappa)}$ with rate functions given by

$$\psi_r(\kappa) = \begin{cases} \frac{1}{4}\left[r^4 - 4r^2\kappa + 3\kappa^2 + 2\kappa^2 \log\frac{r^2}{\kappa}\right], & 0 \leq \kappa < r^2 \\ -\frac{1}{4}\left[r^4 - 4r^2\kappa + 3\kappa^2 + 2\kappa^2 \log\frac{r^2}{\kappa}\right], & r^2 < \kappa \leq 1 \end{cases} . \tag{2-16}$$

By expanding this rate function around its minimum one would expect to recover the CLT describing the typical fluctuations of κ. After a simple derivation one finds that the rate function exhibits a cubic behaviour given by

$$\psi_r(\kappa) \approx \frac{|\kappa - r^2|^3}{6r^2} . \tag{2-17}$$

This is an odd result, as the Gaussian fluctuations are supposed to be quadratic instead of cubic. This clearly indicates that there must be an intermediate regime separating atypical behaviour from typical one.

The whole purpose of this MSc thesis is to explain this discrepancy. In the next chapter we will show that the probability of having K eigenvalues in the domain $\mathcal{D}$ obeys for large N the following

$$\mathcal{P}_r(\kappa, N) \sim \begin{cases} e^{-N^{3/2}\frac{\sqrt{\pi}}{2r}(\kappa - r^2)^2} & , \quad |\kappa - r^2| = \mathcal{O}(N^{-3/4}) \\ e^{-\sqrt{2N}r\psi_I(\kappa)} & , \quad |\kappa - r^2| = \mathcal{O}(N^{-1/2}) \\ e^{-N^2\psi_r(\kappa)} & , \quad |\kappa - r^2| = \mathcal{O}(N^0) \end{cases} , \tag{2-18}$$

which characterizes three regimes: a typical regime, and atypical one, and an intermediate regime that smoothly interpolates between both of them.

3. Intermediate deviation regime for the full eigenvalue statistics in the complex Ginibre ensemble

In this part of the thesis we derive the probability that the index number $\mathcal{N}_{\mathcal{D}}$ will be equal to a number K of eigenvalues within a domain $\mathcal{D} = \{z : z \in \mathbb{C}, |z| \leq r\}$ for the Ginibre ensemble (see figure **3-1**). We denote the number of eigenvalues inside the disk by N_r. This chapter is divided as follows: in section 3.1, we derive exactly the probability of having $N_r = K$ eigenvalues for a finite N and in section 3.2 we determine the typical, atypical and intermediate regimes in the limit of large N.

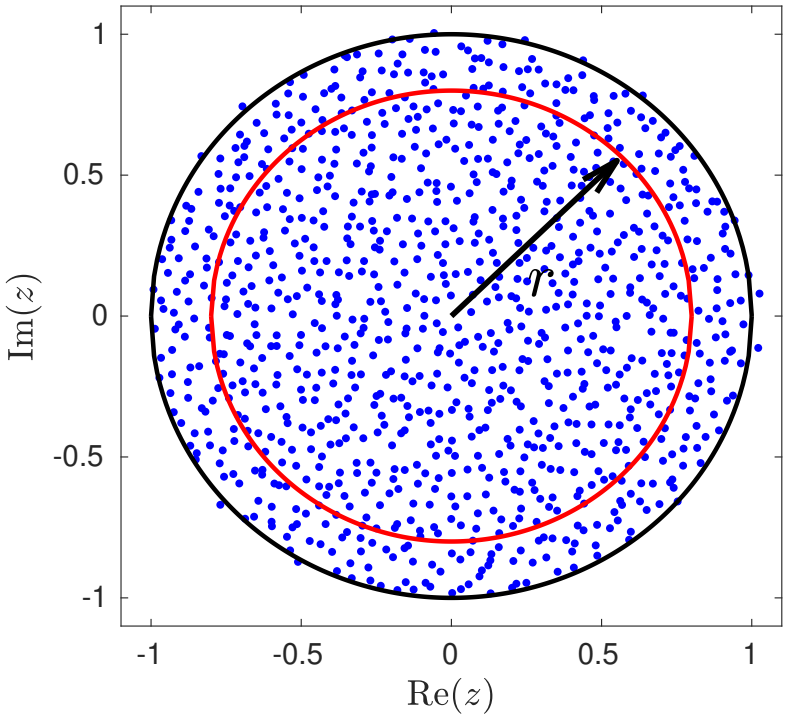

Figure **3-1**.: In this figure we show a number of K eigenvalues for a Ginibre ensemble inside a disk of radius r (red curve). The previous was obtained for a matrix of size $N = 1000$.

3.1. Exact results for finite N

In this section we focus on computing the PDF of having $N_r = K$ eigenvalues inside the disk of radius r, denoted by $P_r(K, N)$. First of all, we introduce the random variable

$$N_r = \sum_{k=1}^{N} \Theta(r - r_i), \tag{3-1}$$

where $r_i = |z_i|$ is the modulus of the i-th eigenvalue and $\Theta(x)$ is the Heaviside step function. To derive the probability $P_r(K, N)$, we express this as an average of the Kronecker delta with respect to the joint PDF given in the eq. (2-8) as $P_r(K, N) = \langle \delta_{N_r,K} \rangle$. Using the definition of the Kronecker delta as an integral and after applying the Vandermonde determinant and the Cauchy-Binet formula (see the appendix A.1 for details), we arrive to the result

$$P_r(K, N) = \int_0^{2\pi} \frac{d\hat{\phi}}{2\pi} \mathrm{e}^{i\hat{\phi}K} \prod_{k=1}^{N} \left[\mathrm{e}^{-i\hat{\phi}} L_k(r) + M_k(r) \right], \tag{3-2}$$

where the terms $L_k(r)$ and $M_k(r)$ are given by

$$M_k(r) = \frac{\int_r^\infty dr' r'^{2k-1} \mathrm{e}^{-Nv(r')}}{\int_0^\infty dr' r'^{2k-1} \mathrm{e}^{-Nv(r')}}, \qquad L_k(r) = \frac{\int_0^r dr' r'^{2k-1} \mathrm{e}^{-Nv(r')}}{\int_0^\infty dr' r'^{2k-1} \mathrm{e}^{-Nv(r')}}. \tag{3-3}$$

Note that $L_k(r)$ and $M_k(r)$ depend on a general spherical potential and are related to each other as $M_k(r) = 1 - L_k(r)$. The Fourier integral given in the equation (3-2) can be solved by using the following identity

$$\prod_{k=1}^{N} \left[e^{-i\hat{\phi}} L_k(r) + M_k(r) \right] = \sum_{\mathcal{A} \subseteq \Omega} e^{-i|\mathcal{A}|\hat{\phi}} L_{\mathcal{A}}(r) M_{\Omega \setminus \mathcal{A}}(r), \tag{3-4}$$

where we introduce the sets Ω and $\mathcal{A}$ with $\Omega = \{1, 2, \cdots, N\}$, and $\mathcal{A}$ any posible subset of Ω. The term $|\mathcal{A}|$ is the cardinality of $\mathcal{A}$ and $f_{\mathcal{A}} = \prod_{K \in \mathcal{A}} f_K$. The term $\sum_{\mathcal{A} \subseteq \Omega}$ indicates that the sum is made over all possible subsets $\mathcal{A} \subseteq \Omega$. Using the eq. (3-4) and expressing the integral in terms of a Kronecker delta, we rewrite eq. (3-2) as

$$P_r(K, N) = \sum_{\mathcal{A} \subseteq \Omega} \delta_{K,|\mathcal{A}|} L_{\mathcal{A}}(r) M_{\Omega \setminus \mathcal{A}}(r). \tag{3-5}$$

From the above equation, we can obtain the cumulant generating function (CGF) of N_r defined as $\chi_r(\mu, N) = \log\langle e^{-\mu N_r} \rangle$, with $\mu = i\hat{\phi}$, and $\langle \cdots \rangle$ the average with respect to the eq. (3-5). The CGF of N_r reads

$$\chi_r(\mu, N) = \log \left(\sum_{K=0}^{N} e^{-\mu K} P_r(K, N) \right) = \sum_{k=1}^{N} \log \left(e^{-\mu} L_k + M_k \right), \tag{3-6}$$

which allows us to obtain the exact cumulants $\langle N_r^p \rangle_c$, where the subscript p is the cumulant order of the random variable N_r. Here, we compute the first four cumulants of N_r, which are displayed

in the following set of equations

$$\begin{aligned} \langle N_r^1\rangle_c &= \sum_{k=1}^{N} L_k, & \langle N_r^2\rangle_c &= \sum_{k=1}^{N} L_k(1-L_k) \\ \langle N_r^3\rangle_c &= \sum_{k=1}^{N} L_k(1+3L_k+2L_k^2), & \langle N_r^4\rangle_c &= \sum_{k=1}^{N} L_k(1-7L_k+12L_k^2-6L_k^3), \end{aligned} \tag{3-7}$$

where we use the short notation $L_k \equiv L_k(r)$ (details for derivations in appendix A.2). This result is rather remarkable as it is valid for a finite N and any general spherical potential $v(r)$. Comparisons between the analytical results from (3-7) and numerical Monte Carlo simulations are presented in section 4.

Using eq.(3-5) for finite N, it is easy to obtain the particular probabilities when we have $K = 0$ and $K = N$ eigenvalues in $\mathcal{D}$, which corresponds to the cumulative distribution function (CDF) of the $r_{\min}$ and $r_{\max}$. Those probabilities read

$$\begin{aligned} P_r(N,N) &= \text{Prob}[r_{\max} \leq r] = \prod_{k=1}^{N} L_k(r) \\ P_r(0,N) &= \text{Prob}[r_{\min} > r] = \prod_{k=1}^{N} M_k(r). \end{aligned} \tag{3-8}$$

For the Ginibre ensemble, $v(r) = r^2$, we have that the exact expressions of $L_k(r)$ and $M_k(r)$ for finite N are

$$M_k(r) = \frac{\Gamma(k, Nr^2)}{\Gamma(k)}, \qquad L_k(r) = 1 - \frac{\Gamma(k, Nr^2)}{\Gamma(k)}, \tag{3-9}$$

where $\Gamma(k,z) = \int_z^\infty t^{k-1}e^{-t}dt$ is the upper incomplete Gamma function.

3.2. The limit of large N

In this section, we compute the behavior of $P_r(K,N)$ for the Ginibre ensemble for large N. Firstly, we use the expression of the probability distribution function in eq. (3-2) in terms of the functions $L_k(r)$ and $M_k(r)$ which are found in the formulas (3-9). Clearly, we can rewrite the PDF given in (3-2) as

$$P_r(K,N) = \int_{-i\pi}^{i\pi} \frac{d\mu}{2\pi i} \exp\left[\mu K + \sum_{k=1}^{N} \log\left(e^{-\mu}L_k + M_k\right)\right]. \tag{3-10}$$

Note that the sum term is nothing but the cumulant generating function (CGF), which is given in the eq. (3-6). To derive the asymptotic behavior of the PDF given in eq. (3-10), we set $k = xN$ and use the Euler-Mclaurin formula [11] for large N which allows us to express the CGF $\chi_r(\mu, N)$ as an integral such that eq.(3-10) in the asymptotic limit reads

$$\mathcal{P}_r(\kappa, N) = \int_{\mathcal{C}} \frac{d\mu}{2\pi i} \exp\left[N\kappa\mu + N\int_0^1 dx \log\left(e^{-\mu}L_{xN}(r) + M_{xN}(r)\right)\right], \tag{3-11}$$

where $\kappa = N_r/N$. This result can be seen as an inverse Laplace integral where $\mathcal{C}$ is the Bromwich contour (see the appendix B.1 and figure **B-1**). In the next section, we solve the PDF given in eq. (3-11) in the three mentioned regimes: (i) typical, (ii) intermediate and (iii) atypical.

3.2.1. Regime of typical fluctuations

Here, we present the solutions of the PDF given in eq. (3-11) in the regime of typical fluctuations. Moreover, we compute the mean and variance for large N and we prove that the rate function has a quadratic behavior near its mean. We start solving equation (3-11) by using the saddle point method which leads us to the formulas

$$\begin{aligned} &\mathcal{P}_r(\kappa, N) \asymp \exp(-N\Phi_r(\kappa, N)) \\ &\Phi_r(\kappa, N) = \min_\mu(\mu\kappa - \Xi_r(\mu, N)) \\ &\Xi_r(\mu, N) = \int_0^1 dx \log\left(\mathrm{e}^{-\mu} L_{xN}(r) + M_{xN}(r)\right), \end{aligned} \tag{3-12}$$

where the term $N\Xi_r(\mu, N)$ is the CGF in the limit of large N. Notice that $\Phi_r(\kappa, N)$ has a minimum at $\mu = 0$. This point corresponds to the maximum of the probability in which κ fluctuates around its typical value and therefore the Lagrange multiplier μ becomes ineffective. Doing and expansion of $\Xi_r(\mu, N)$ in powers of μ around zero up to second order, leads us to

$$\Phi_r(\kappa, N) = \min_\mu \left[\mu\left(\kappa - \frac{d}{d\mu}\Xi_r(\mu, N)\Big|_{\mu=0}\right) - \frac{\mu^2}{2}\frac{d^2}{d\mu^2}\Xi_r(\mu, N)\Big|_{\mu=0} + \mathcal{O}(\mu^3)\right]. \tag{3-13}$$

Now, solving the above equation we find that the minimum $\mu = \mu*$ is

$$\mu* = \frac{1}{\frac{d^2}{d\mu^2}\Xi_r(\mu, N)\Big|_{\mu=0}}\left(\kappa - \frac{d}{d\mu}\Xi_r(\mu, N)\Big|_{\mu=0}\right). \tag{3-14}$$

Plugging equation (3-14) into the eq. (3-13), we obtain that

$$\Phi_r(\kappa, N) = \frac{1}{2\frac{d^2}{d\mu^2}\Xi_r(\mu, N)\Big|_{\mu=0}}\left(\kappa - \frac{d}{d\mu}\Xi_r(\mu, N)\Big|_{\mu=0}\right)^2. \tag{3-15}$$

This result proves that the PDF has a Gaussian behavior in the typical regime given by

$$\mathcal{P}_r(\kappa, N) \asymp \exp\left(\frac{1}{2}\frac{(\kappa - \langle\kappa\rangle)^2}{\mathrm{Var}(\kappa)}\right), \tag{3-16}$$

where the mean and the variance behave asymptotically as in the following formulas

$$\langle\kappa\rangle \sim \int_0^1 dx L_{xN}(r), \qquad \mathrm{Var}(\kappa) \sim \frac{1}{N}\int_0^1 dx L_{xN}(r)(1 - L_{xN}(r)). \tag{3-17}$$

Since these integrals depend on the upper incomplete gamma function, we use the asymptotic behavior of $L_{xN}(r)$ and $M_{xN}(r)$ obtained with Laplace method (see appendix B.2) that allows

us to compute easily the above integrals (see appendix B.3). Then, we have that the mean and variance of κ for large N have the form

$$\langle\kappa\rangle \sim r^2, \qquad \mathrm{Var}(\kappa) \sim \frac{r}{N^{3/2}\sqrt{\pi}}. \tag{3-18}$$

Gathering the results, we obtain that the PDF of κ in the typical regime for large N is

$$\mathcal{P}_r(\kappa, N) \asymp \exp\left[-\frac{N^{3/2}\sqrt{\pi}}{2r}\left(\kappa - r^2\right)^2\right], \tag{3-19}$$

where this result is found in the first line of eqs. (2-18).

3.2.2. Regime of intermediate fluctuations

In this section, we solve the PDF given in eq. (3-11) in the intermediate regime, where in this case we keep the dependence with the parameter μ in the CGF, $N\Xi_r(\mu, N)$, with $\Xi_r(\mu, N)$ given in the third line of the equations (3-12). Since the fluctuations in this regime are of the order $|\kappa - r^2| = \mathcal{O}(N^{-1/2})$, we use the asymptotic expression of $L_{xN}(r)$ and $M_{xN}(r)$ when $\kappa \sim r^2$, which are given in terms of the complementary error function (see appendix B.2) as it is shown below

$$L_{xN}(r) \sim \frac{1}{2}\mathrm{erfc}\left[\sqrt{2N}(\sqrt{x} - r)\right], \tag{3-20}$$

where $M_{xN}(r) = 1 - L_{xN}(r)$. Now, we use the result given in the eq. (3-20) and the identity $\mathrm{erfc}(x) + \mathrm{erfc}(-x) = 2$ to manipulate the cumulant generating function which leads us to that the PDF given in eq. (3-11) can be written as (see appendix C for details)

$$\mathcal{P}_r(\kappa, N) \sim \int_{\mathcal{C}} \frac{d\mu}{2\pi i} \exp\left[-\sqrt{2N}r\left(\mu y + \chi(\mu)\right)\right], \quad y = \sqrt{\frac{N}{2r^2}}(\kappa - r^2), \tag{3-21}$$

with scaling function

$$\chi(\mu) \equiv \int_0^\infty du \log\left[1 + \sinh^2\left(\frac{\mu}{2}\right)\mathrm{erfc}(u)\mathrm{erfc}(-u)\right], \tag{3-22}$$

which is related with the CGF via $\sqrt{2N}r\chi(\mu)$ in the regime of intermediate fluctuations. From this expression we can see immediately properties about the cumulants of $\mathcal{P}_r(\kappa, N)$. For instance, the Taylor expansion of the expression (3-22) tells us that the odd cumulants vanish due to the fact that $\chi(\mu)$ is an even function with respect to μ. Next, using the saddle point method we solve the integral given in (3-21), which yields the main result: the intermediate rate function, $\psi_I(k)$, that characterizes the fluctuations in the intermediate regime and it is shown in the second line of the equation below

$$\begin{aligned} \mathcal{P}_r(\kappa, N) &\asymp \exp(-\sqrt{2N}r\psi_I(\kappa)) \\ \psi_I(\kappa) &= \min_{\mu\in\mathbb{R}}\{y\mu + \chi(\mu)\}, \quad y = \sqrt{\frac{N}{2r^2}}(\kappa - r^2). \end{aligned} \tag{3-23}$$

Looking closely at the previous expression, it seems difficult to obtain a more explicit expression of the rate function. However, we can obtain the asymptotic behavior of this function when $\mu \to 0$

and $\mu \to \infty$ by using the asymptotical form of $\chi(\mu)$ in the mentioned limit situations, which is (for details see appendix C.1 and appendix C.2)

$$\chi(\mu) \sim \begin{cases} \frac{1}{2\sqrt{2\pi}}\mu^2 & , \quad \mu \to 0 \\ \\ \frac{2}{3}|\mu|^{3/2} & , \quad \mu \to \infty \end{cases} \tag{3-24}$$

and allows us to prove that the intermediate rate function interpolates between the typical and atypical regimes. Firstly, for small fluctuations we substitute the limit behavior of $\chi(\mu)$ when $\mu \to 0$ in the second line of the equation (3-23), obtaining that

$$\psi_I(y) \sim \min_{\mu\in\mathbb{R}}\left\{\mu y + \frac{\mu^2}{2\sqrt{2\pi}}\right\}, \tag{3-25}$$

where the minimum is found at $\mu* = -y\sqrt{2\pi}$. Then, evaluating the eq. (3-25) at μ^*, we obtain that the intermediate rate function for small μ has a quadratic behavior given by

$$\psi_I(y) \sim y^2\sqrt{\frac{\pi}{2}}, \qquad y = \sqrt{\frac{N}{2r^2}}(\kappa - r^2). \tag{3-26}$$

Expressing the eq. (3-26) in terms of κ and r^2, and replacing it in the first line of equations (3-23), we obtain that the PDF of κ for small μ is

$$\mathcal{P}_r(\kappa, N) \asymp e^{-N^{3/2}\frac{\sqrt{\pi}}{2r}(\kappa - r^2)^2},$$

where this result matches with the obtained in the typical regime in the previous section given in the eq. (3-19).
Secondly, we prove that the intermediate rate function connects with the regime of large fluctuations. We use the asymptotic behavior of the scaling function $\chi(\mu)$ for large $|\mu|$ given in eq. (3-24) and obtain the following minimization problem

$$\psi_I(y) \sim \min_{\mu\in\mathbb{R}}\left\{\mu y + \frac{2}{3}|\mu|^{3/2}\right\}. \tag{3-27}$$

The point $\mu = \mu*$ that minimizes the above expression is $\mu* = -\text{sign}(y)y^2$, which points out that the intermediate rate function in this case behaves as

$$\psi_I(y) \sim \frac{|y|^3}{3}, \qquad y \to \pm\infty. \tag{3-28}$$

Plugging $y = \sqrt{\frac{N}{2r^2}}(\kappa - r^2)$ into the above equation shows us that the eq. (3-28) matches with the cubic behavior of the large rate function given in the expression (2-17). Moreover, the PDF of κ in the tails of the intermediate regime has the form

$$\mathcal{P}_r(\kappa, N) \asymp \exp\left(-N^2\frac{|k - r^2|^3}{6r^2}\right). \tag{3-29}$$

Finally, we conclude that an intermediate phase exist and it is able to connect the regimes of central and large fluctuations.

3.2.3. Regime of atypical fluctuations

In this section we focus on the large fluctuations which are of order $|\kappa - r^2| = \mathcal{O}(1)$. We can obtain those results if we rescale $\mu = -\lambda N$ with $\lambda = \mathcal{O}(1)$ in eq. (3-11). In this regime, we employ the uniform asymptotic expansion of the upper incomplete Gamma function (for more details see [35]) to rewrite $M_{xN}(r)$ and $L_{xN}(r)$ as

$$\begin{aligned} M_{xN}(r) &= \mathrm{e}^{-N(r^2 - x - x\log\frac{r^2}{x}) + o(N)}, \qquad & x \leq r^2 \\ M_{xN}(r) &= 1 - \mathrm{e}^{-N(r^2 - x - x\log\frac{r^2}{x}) + o(N)}, \qquad & x \geq r^2, \end{aligned} \tag{3-30}$$

where $L_{xN}(r) = 1 - M_{xN}(r)$. After the rescaling, we use the saddle point method to solve the integral given in the eq. (3-11), obtaining the following formulas

$$\begin{aligned} \mathcal{P}_r(\kappa, N) &\asymp \exp[-N^2\psi_r(\kappa)] \\ \psi_r(\kappa) &= \min_\lambda\{\lambda\kappa - \Xi_r(\lambda)\} \\ \Xi_r(\lambda) &= \frac{1}{N}\int_0^1 dx \log\left[\mathrm{e}^{N\lambda}L_{xN}(r) + M_{xN}(r)\right] \\ \kappa &= \int_0^1 dx \frac{\mathrm{e}^{N\lambda^*}L_{xN}(r)}{\mathrm{e}^{N\lambda^*}L_{xN}(r) + M_{xN}(r)}. \end{aligned} \tag{3-31}$$

The first line in the above equation is the large deviation principle with speed rate N^2 and rate function $\psi_r(\kappa)$. The term $N^2\Xi_r(\lambda)$ is the cumulant generating function (CGF) in the atypical regime for large N and the fourth line is the saddle point equation. Now, we introduce the notation

$$\varphi_r(x) = r^2 - x - x\log\frac{r^2}{x}, \tag{3-32}$$

which is a positive convex function of $x \in [0, 1]$ with a minimum at $x = r^2$. To compute the rate function, we insert the expressions given in the eqs. (3-30) into the scaling function given in the third line of the eqs. (3-31), which leads us to

$$N\Xi_r(\lambda) \sim \int_0^{r^2} dx \log[e^{N\lambda}(1 - e^{-N\varphi_r(x))}) + e^{-N\varphi_r(x)}] + \int_{r^2}^1 dx \log[e^{N(\lambda - \varphi_r(x))} + 1 - e^{-N\varphi_r(x)}]. \tag{3-33}$$

Note that this function has two behaviors depending on the sign of λ. For $\lambda > 0$, we can see that the right integral contributes to the solution only for values of x when $(\lambda - \varphi_r(x)) \geq 0$. Thus, the right integral will be different from zero if we integrate from r^2 to $\min\{1, F(\lambda, r)\}$, where $F(\lambda, r)$ is the solution in x, for $x \geq r^2$, of the equation $(\lambda - \varphi_r(x)) = 0$. Thus, we have that

$$\Xi_r(\lambda) \sim r^2\lambda + \int_{r^2}^{\min\{1, F(\lambda, r)\}} (\lambda - \varphi_r(x))dx, \qquad \lambda > 0. \tag{3-34}$$

Next, solving the equation for the saddle point λ^* given in the fourth line of eqs. (3-31) after taking into account the different cases in eqs. (3-30), we obtain that λ^* is such that $\kappa = \min\{1, F(\lambda^*, r)\}$ with $r^2 \leq \kappa \leq 1$ (see appendix D for details). Therefore, the solution of the second line given in the eqs. (3-31) yields the rate function for the right tail

$$\psi_r(\kappa) = \frac{1}{4}\left[-r^4 + 4r^2\kappa - 3\kappa^2 - 2\kappa^2\log\frac{r^2}{\kappa}\right], \qquad r^2 \leq \kappa \leq 1. \tag{3-35}$$

For $\lambda < 0$ we do a similar analysis, where we have that

$$\Xi_r(\lambda) \sim r^2\lambda - \int_{\kappa}^{r^2} (\lambda + \varphi_r(x))dx, \quad \lambda < 0, \tag{3-36}$$

for $\kappa = \max\{0, G(\lambda^*, r)\}$ and $G(\lambda, r)$ is the solution in x of the equation $(\lambda+\varphi_r(x)) = 0$ (for details see appendix D). This allows us to compute the rate function for the left tail expressed as

$$\psi_r(\kappa) = \frac{1}{4}\left[r^4 - 4r^2\kappa + 3\kappa^2 + 2\kappa^2 \log\frac{r^2}{\kappa}\right], \quad 0 \leq \kappa \leq r^2. \tag{3-37}$$

Thus, with the rate functions given in the eqs (3-35) and (3-37) we recover the result of [34] in the atypical regime.
Using equations (3-35) and (3-37) we can obtain the particular rate functions of the CDF of $r_{\min}$ and $r_{\max}$ when $\kappa = 0$ or $\kappa = 1$, respectively. For the first one, we have that

$$\begin{aligned} \psi_r(\kappa = 1) &= -\frac{1}{N^2}\log \text{Prob}[r_{\max} \leq r] \\ &= -\frac{1}{4}(r^4 - 4r^2 + 3) - \log(r), \end{aligned} \tag{3-38}$$

where this result matches with the one given in the first line of eq. (2-14) (making $w = r$). For the CDF of $r_{\min}$, we arrive to the following form

$$\begin{aligned} \psi_r(\kappa = 0) &= -\frac{1}{N^2}\log \text{Prob}[r_{\max} \leq r] \\ &= \frac{1}{4}r^4. \end{aligned} \tag{3-39}$$

Finally, we were able to derive the three different regimes where the most remarkable result is the existence of the intermediate phase which interpolates smoothly the regimes of typical and atypical fluctuations.

4. Comparison with Monte Carlo simulations

In this chapter we show a comparison between the exact results for the first four cumulants $\langle N_r^p \rangle_c$, $1 \leq p \leq 4$, from equations (3-7) with Monte Carlo simulations. These observables are related with the typical fluctuations of N_r and they can be obtained by a standard Metropolis algorithm to simulate the joint PDF of the Ginibre ensemble eq. (2-8). These results are displayed in the figure **4-1** for $N = 100$ eigenvalues and $1{,}2 \times 10^7$ Monte Carlo steps which shows us a good agreement with respect to the theoretical expressions.

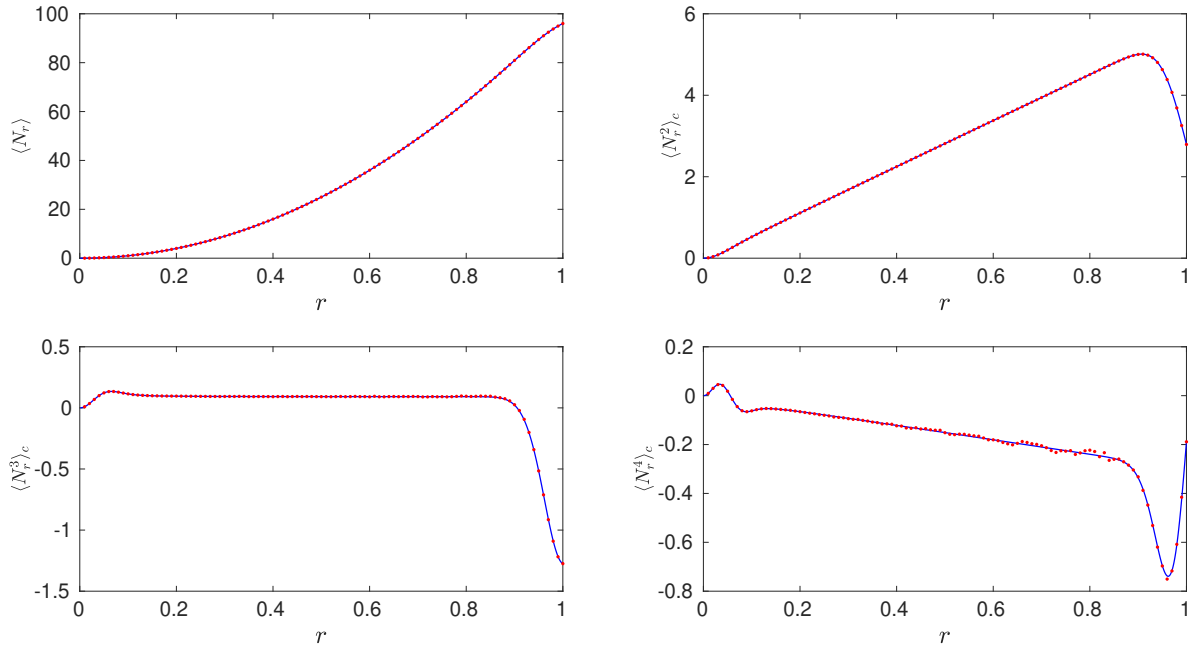

Figure **4-1**.: In this figure is compared the theoretical first four cumulants of N_r as a function of r (solid blue line) with Monte Carlo simulations (red dots). The simulations were performed for $N = 100$ and averaging over $1{,}2 \times 10^7$ samples

Since we want to go beyond the first four cumulants and sample the intermediate and large regime fluctuations, we need a numerical method capable of exploring probabilities which are far from the expected value [36]. This can be done by an "importance" sampling approach as is found in [37]. The idea behind this is the following: we need that the atypical values of κ become "typical" with respect to an auxiliary distribution. This later is introduced through the following auxiliary joint

PDF

$$P^{\beta}_{\text{joint}}(z_1,...,z_N) = \frac{e^{-\beta\sum_{i=1}^{N}\Theta(r-|z_i|)}}{Z_\beta}\prod_{i<j}|z_i-z_j|^2\prod_{k=1}^{N}e^{-NV(z_k)}, \tag{4-1}$$

where β plays a role analogous to the inverse of temperature in statistical physics, where the difference is that this parameter may have positive or negative values. The term $e^{-\beta\sum_{i=1}^{N}\Theta(r-|z_i|)}$ is a Boltzmann factor and Z_β is a normalization constant [37]. Now, let us introduce the definitions of the probability of having $N_r = \kappa N$ eigenvalues below the circle of radius r in the unbiased ($\beta = 0$) and the biased ($\beta \neq 0$) problem as

$$\begin{aligned}\frac{1}{N}\mathcal{P}_r(\kappa = K/N, N) &= \sum_{\vec{z}} P_{\text{joint}}(z_1,...,z_N)\delta_{N_r,K}\\ \frac{1}{N}\mathcal{P}^{\beta}_r(\kappa = K/N, N) &= \sum_{\vec{z}} P^{\beta}_{\text{joint}}(z_1,...,z_N)\delta_{N_r,K},\end{aligned} \tag{4-2}$$

where P_{joint} is given in the eq. (2-8) and P^{β}_{joint} is found in the eq. (4-1). The sum is performed over all possible values of $\vec{z} = (z_1, z_2, ..., z_N)$. From the eqs. (4-2) we can easily prove that

$$\mathcal{P}_r(\kappa, N) = e^{\beta N\kappa} Z_\beta \mathcal{P}^{(\beta)}_r(\kappa, N). \tag{4-3}$$

The role of β is to force the atypical values of κ with respect to the unbiased problem to become typical in the auxiliary problem. The latter is known as "reweighting"[37, 36]. With this in mind, we perform a Monte Carlo simulation with respect to the auxiliary joint PDF given in the eq. (4-1) for a fixed β to construct the histogram of κ in the biased problem. Therefore, if we use the equation (4-3), we can obtain the PDF of κ in a region where it is atypical with respect to the unbiased problem up to a normalization constant. Consequently, if we perform the simulations for different values of β, we could get $\mathcal{P}_r(\kappa, N)$ over its full support [37]. The positive values of β will allow us to know the distribution of κ to the left of its typical value, while the negative ones will lead us to know the distribution of κ to the right of the expected value. Note that small values of $|\beta|$ yields histograms in a region that overlaps with respect to the original distribution. The latter is necessary to be able to "glue" the histograms using the eq. (4-3), where Z_β allows us the "gluing" process. Therefore, the set of values of β must be chosen in such a way that the histograms overlap each other, and thus we can obtain $\mathcal{P}_r(\kappa, N)$ properly normalised in the three regimes: typical, intermediate and atypical [37].

Monte Carlo simulations were carried out for a system of $N = 500$ eigenvalues with a fixed radius $r = 0.5$. The theoretical and numerical results of $-\frac{1}{N}\log\mathcal{P}_r(\kappa, N)$ are shown in the figure **4-2**, where we can see good agreement between the three theoretical regimes found in this thesis: the typical (black solid line), atypical (red solid line), and intermediate (green solid line) with the numerical simulations (solid blue circular markers).

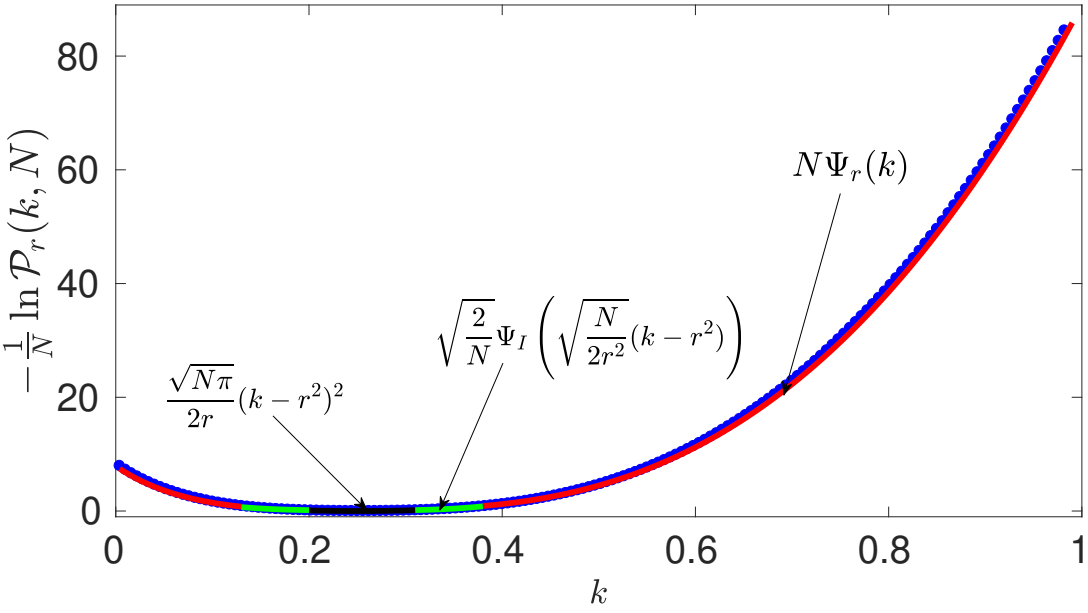

Figure **4-2**.: This figure shows the numerical results of $-\frac{1}{N}\log\mathcal{P}_r(\kappa,N)$ obtained by "importance" sampling tecniques (blue circular markers) and the theoretical results for typical (solid black curve), intermediate (solid green curve) and atypical (solid red curve) fluctuations of κ for $N=500$ eigenvalues and $r=1/2$. The simulations were performed for a set of values of β between -333 and 117 in steps of 4.5 and using 2.8×10^5 samples.

5. Conclusions and outlook

To conclude, we have provided rather complete understanding of the statistical behavior for the number N_r of eigenvalues of $N \times N$ complex Ginibre matrices inside a disk of radius r. For typical fluctuations, we have obtained exact expressions, valid for any N, of the distribution and also for the first 4 cumulants. We want to highlight that this result is also valid for any general spherical potential.

In the limit of large N, we find the distribution $\mathcal{P}_r(\kappa = K/N, N)$ obeys different probability laws depending on three different scales associated with the fluctuations of κ: (i) a regime of typical fluctuations described by a Gaussian distribution, (ii) a large fluctuations regime which is characterized by a large deviation function, and (iii) a regime of intermediate fluctuations. The latter that smoothly interpolates between the typical and atypical regimes. Our results were throughly compared with Monte Carlo simulations, showing excellent agreement

This intermediate phase is a novel result because it does not exist in the fluctuations of the index number in $\beta-$Gaussian, $\beta-$Cauchy and $\beta-$Wishart ensembles, where in those ensembles, the large deviation regime matches with the regime of typical fluctuations [28, 29] . Even though an intermediate deviation regime has been observed in other similar situations, as is the case of the statistics of the eigenvalue with the largest modulus $r_{\max}$ in the complex Ginibre ensemble [16].

We hope that our results may shed some light into the description of real physical systems. For instance, for a system of 2-d rotating fermions in a trap, the FCS of the index number derived in this work is connected with some physical quantities, juts like the entanglement entropy with the variance of N_r [38]

The results of this work motivate us to study the full counting statistics of N_r in other ensembles, such as the real or the symplectic Ginibre ensemble, or the problem of the mismatch between the typical and large regimes in the 1d Coulomb gas in the presence of a general external convex potential [39], which could be explained due to the existence of an intermediate phase. All these problems will motivate future projects.

A. Derivation of exact results for finite N

A.1. Exact probability of having $N_r = K$ eigenvalues

First, we employ the definition of the joint probability density function (PDF) in the Ginibre ensemble given in eq. (2-8). Then, we derive the probability of having exactly K eigenvalues inside the domain $\mathcal{D} = \{z : z \in \mathbb{C}, |z| \leq r\}$ as

$$\text{Prob}[N_r = K] = P_r(K, N) = \langle \delta_{N_r}, K \rangle, \tag{A-1}$$

where $\langle \cdots \rangle$ denotes the average with respect to the joint PDF of the Ginibre ensemble. Thus, the integral for $P_r(K, N)$ is

$$P_r(K, N) = \frac{1}{Z_N} \int d^2 z_1 \cdots \int d^2 z_N \prod_{i<j} |z_i - z_j|^2 \prod_{k=1}^{N} \left[\mathrm{e}^{-NV(z_k)} \right] \delta_{N_r, K}, \tag{A-2}$$

where $\int d^2 z = \int \int dx dy$. Now, we compute the partition function Z_N using the Vandermonde determinant which is given by $\prod_{i<j}(z_i - z_j) = \det_{1 \leq i,j \leq N}(z_i^{j-1})$, as it is shown below

$$Z_N = \int d^2 z_1 \cdots \int d^2 z_N \det_{1 \leq i,j \leq N} \left(z_i^{j-1} \mathrm{e}^{-NV(|z_i|)} \right) \det_{1 \leq i,j \leq N} \bar{z}_i^{j-1} \left(\mathrm{e}^{-NV(|z_i|)} \right). \tag{A-3}$$

To simplify this integral, we use the Cauchy- Binet identity given by

$$\int \left[\prod_{i=1}^{N} w(x_i) dx_i \right] \det_{1 \leq i,j \leq N} [\phi_i(x_j)] \det_{1 \leq i,j \leq N} [\psi_i(x_j)] = N! \det_{1 \leq i,j \leq N} \left(\int dx w(x) \phi_i(x) \psi_j(x) \right), \tag{A-4}$$

which leads us to

$$Z_N = N! \det_{1 \leq i,j \leq N} \left(\int d^2 z \mathrm{e}^{-Nv(|z|)} z^{i-1} \bar{z}^{j-1} \right), \tag{A-5}$$

whose main advantage is that we went from solving an integral of N variables to solve an integral of one variable. Now, we solve the integral term of the above expression in polar coordinates as

$$\begin{aligned} \int d^2 z \mathrm{e}^{-Nv(|z|)} z^{i-1} \bar{z}^{j-1} &= \int_0^{2\pi} d\theta \mathrm{e}^{i\theta(i-j)} \int_0^{\infty} dr r^{j+i-1} \mathrm{e}^{-NV(r)} \\ &= 2\pi \delta_{ij} \int_0^{\infty} dr r^{2i-1} \mathrm{e}^{-NV(r)}. \end{aligned} \tag{A-6}$$

Thus, the partition function has the form

$$Z_N = N! \prod_{k=0}^{N-1} h_k, \quad h_k = 2\pi \int_0^{\infty} dr r^{2k-1} \mathrm{e}^{-NV(r)}. \tag{A-7}$$

The next step is to compute $P_r(K,N)$. Then, we focus on the numerator term in equation (A-2), where we use the integral definition of the Kronecker delta $(2\pi)^{-1}\int_0^{2\pi} d\theta \mathrm{e}^{i\theta(l-k)} = \delta_{l,k}$. Therefore

$$P_r(K,N) = \frac{1}{Z_N}\int_0^{2\pi}\frac{d\hat{\phi}}{2\pi}\mathrm{e}^{i\hat{\phi}K}\int d^2z_1\cdots\int d^2z_N\prod_{i<j}|z_i-z_j|^2\prod_{k=1}^{N}\left[\mathrm{e}^{-NV(z_k)}\right]\mathrm{e}^{-i\hat{\phi}\sum_{i=1}^{N}\Theta(r-|r_i|)}. \tag{A-8}$$

If we write the exponential term as $\mathrm{e}^{-i\hat{\phi}\sum_{i=1}^{N}\Theta(r-|r_i|)} = \prod_{k=1}^{N}\mathrm{e}^{-i\Theta(r-|r_i|)}$, we can use again the Vandermonde determinant and the Cauchy-Binet formula to rewrite the eq. (A-8) as follows

$$P_r(K,N) = \frac{N!}{Z_N}\int_0^{2\pi}\frac{d\hat{\phi}}{2\pi}\mathrm{e}^{i\hat{\phi}K}\det_{1\le i,j\le N}\left(\int d^2z\mathrm{e}^{-nv(|z|)-i\hat{\phi}\Theta(r-|z|)}z^{i-1}\bar{z}^{j-1}\right), \tag{A-9}$$

where the integral term has the following solution

$$\int d^2z\mathrm{e}^{-nv(|z|)-i\hat{\phi}\Theta(r-|z|)}z^{i-1}\bar{z}^{j-1} = 2\pi\delta_{ij}\int_0^{\infty}dr'r'^{2i-1}\mathrm{e}^{-Nv(r')-i\hat{\phi}\Theta(r-r')}.$$

Now, we introduce the definition

$$h_k(r,\hat{\phi}) \equiv 2\pi\int_0^{\infty}dr'r'^{2k-1}\mathrm{e}^{-Nv(r')-i\hat{\phi}\Theta(r-r')}, \tag{A-10}$$

which allows us to write $P_r(K,N)$ in a compact form given by

$$P_r(K,N) = \int_0^{2\pi}\frac{d\hat{\phi}}{2\pi}\mathrm{e}^{i\hat{\phi}K}\prod_{k=0}^{N-1}\frac{h_k(r,\hat{\phi})}{h_k}. \tag{A-11}$$

Splitting the integral given in eq. (A-10) as $\int_0^{r^2}dr' + \int_{r^2}^{1}dr'$, we can express finally $P_r(K,N)$ as it is shown below

$$P_r(K,N) = \int_0^{2\pi}\frac{d\hat{\phi}}{2\pi}\mathrm{e}^{i\hat{\phi}K}\prod_{k=1}^{N}\left[\mathrm{e}^{-i\hat{\phi}}L_k(r) + M_k(r)\right], \tag{A-12}$$

where we introduce the functions $L_k(r)$ and $M_k(r)$ as

$$M_k(r) = \frac{\int_r^{\infty}dr'r'^{2k-1}\mathrm{e}^{-Nv(r')}}{\int_0^{\infty}dr'r'^{2k-1}\mathrm{e}^{-Nv(r')}}, \qquad L_k(r) = \frac{\int_0^{r}dr'r'^{2k-1}\mathrm{e}^{-Nv(r')}}{\int_0^{\infty}dr'r'^{2k-1}\mathrm{e}^{-Nv(r')}}. \tag{A-13}$$

A.2. Cumulants for finite N

The first four cumulants of $P_r(K,N)$ for a general potential can be computed exactly. To do this, we remind that they are derived from the cumulant generating function (CGF)

$$\chi_r(\mu,N) = \log\left(\sum_{K=0}^{N}e^{-\mu K}P_r(K,N)\right) = \sum_{k=1}^{N}\log\left(e^{-\mu}L_k + M_k\right), \tag{A-14}$$

by a Taylor expansion around $\mu = 0$ up to fourth order as it is shown in the following result

$$\begin{aligned}\chi_r(\mu, N) &= \sum_{k=1}^{N} \log\left(e^{-\mu} L_k + M_k\right) \\ &= -\mu \sum_{k=1}^{N} L_k - \frac{\mu^2}{2} \sum_{k=1}^{N} L_k(1 - L_k) - \frac{\mu^3}{6} \sum_{k=1}^{N} L_k(1 + 3L_k + 2L_k^2) \\ &\quad + \frac{\mu^4}{24} \sum_{k=1}^{N} L_k(1 - 7L_k + 12L_k^2 - 6L_k^3) + \mathcal{O}(\mu^5)\end{aligned} \tag{A-15}$$

where we use the short notation $L_k \equiv L_k(r)$. From the above expression we identify the first four cumulants, which are shown in the set of equations given in eq. (3-7). Note that these cumulants are valid for any general spherical potential $v(r)$.

B. Useful results for large N

B.1. Inverse Laplace integral

The formula for inverse Laplace integrals is given by

$$F(t) = \frac{1}{2\pi i} \int_{a-i\infty}^{a+i\infty} e^{st} f(s) ds, \quad t > 0 \tag{B-1}$$

where the integration path is an infinite straight line on the imaginary axis, $\mathrm{Re}(s) = a$. The function $f(s)$ is a complex function and the contour $\mathcal{C} = \{s \in \mathbb{C} | s = a + iy, y \in \mathbb{R}\}$ is called the *Bromwich contour* (see figure **B-1**). We choose the constant a such that all finite singularities of $f(s)$ are to the left of the real part of $\mathcal{C}$ to guarantee convergence [40]. The above integral can be solved by complex analysis integration methods such as the residue theorem or saddle point method. The integral (B-1) is known too as *Bromwich integral* or *Fourier-Mellin theorem* [40].

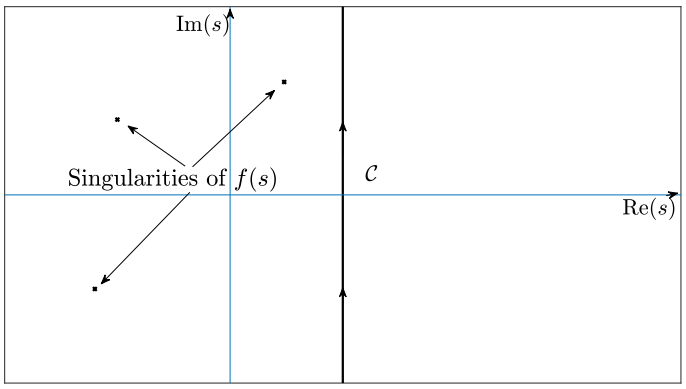

Figure **B-1**.: In this figure we can see the Bromwich contour $\mathcal{C}$, given by the solid black line, and the singularities of $f(s)$ which are to the left of $\mathcal{C}$.

B.2. Asymptotic behavior of $L_{xN}(r)$ and $M_{xN}(r)$

In this appendix section we find the asymptotic behavior of $L_{xN}(r)$ and $M_{xN}(r)$ using the Laplace method. This mathematical derivation was performed by [16]. Firstly, we focus only in $M_{xN}(r)$ because $L_{xN}(r)$ can be easily determined with $L_{xN}(r) = 1 - M_{xN}(r)$. We have

$$M_{xN}(r) = \frac{\Gamma(Nx, Nr^2)}{\Gamma(xN)}. \tag{B-2}$$

Now, we manipulate the above expression as shown below

$$\begin{aligned}\Gamma(Nx, Nr^2) &= \int_{Nr^2}^{\infty} t^{Nx-1}e^{-t}dt \\ &= \int_0^{\infty} t^{Nx-1}e^{-t}dt - \int_0^{Nr^2} t^{Nx-1}e^{-t}dt,\end{aligned} \tag{B-3}$$

which lead us to that $M_{xN}(r)$ can be expressed as

$$\frac{\Gamma(Nx, Nr^2)}{\Gamma(Nx)} = 1 - \frac{\int_0^{Nr^2} t^{Nx-1}e^{-t}dt}{\Gamma(Nx)}. \tag{B-4}$$

Now, we only focus on the integral given in the numerator and proceed to do the variable change $t = Nr'^2$, which leads us to that

$$\begin{aligned}\int_0^{Nr^2} t^{Nx-1}e^{-t}dt &= 2N^{Nx}\int_0^r \frac{1}{r'}e^{-N(r'^2-2x\log r')}dr' \\ &= 2N^{Nx}\int_0^r g(r')e^{-N(\varphi(r'))}dr',\end{aligned} \tag{B-5}$$

where $\varphi(r') = r'^2 - 2x\log r'$ and $g(r') = \frac{1}{r'}$. Thus, we proceed to solve the above integral with the Laplace method, where we have that the minimun of $\varphi(r')$ is found at $r' = \sqrt{x}$. Then, we compute the following integral taking account if $\sqrt{x} \leq r'$ or $\sqrt{x} \geq r'$. First, the case when $\sqrt{x} \leq r'$

$$\begin{aligned}\int_0^r g(r')e^{-N(\varphi(r'))}dr' &\sim g(r_o)e^{-N\varphi(r_0)}\sqrt{\frac{2}{N\varphi''(r_0)}}\int_{-\sqrt{\frac{N\varphi(r_o)''}{2}}(\sqrt{x})}^{\sqrt{\frac{N\varphi(r_o)''}{2}}(r-\sqrt{x})} e^{-y^2}dy \\ &\sim g(r_o)e^{-N\varphi(r_0)}\sqrt{\frac{2}{N\varphi''(r_0)}}\int_{-\infty}^{\sqrt{\frac{N\varphi(r_o)''}{2}}(r-\sqrt{x})} e^{-y^2}dy \\ &\sim g(r_o)e^{-N\varphi(r_0)}\sqrt{\frac{2}{N\varphi''(r_0)}}\int_{\sqrt{\frac{N\varphi(r_o)''}{2}}(\sqrt{x}-r)}^{\infty} e^{-y^2}dy,\end{aligned} \tag{B-6}$$

which allows us to express the above result in terms of the complementary error function as

$$\int_0^r g(r')e^{-N(\varphi(r'))}dr' \sim g(r_o)e^{-N\varphi(r_0)}\sqrt{\frac{\pi}{2N\varphi''(r_0)}}\text{erfc}\left(\sqrt{\frac{N\varphi(r_o)''}{2}}(\sqrt{x}-r)\right). \tag{B-7}$$

Thus, the integral given in eq. (B-5) can be approximated by

$$\int_0^{Nr^2} t^{Nx-1}e^{-t}dt \sim 2N^{Nx}g(r_o)e^{-N\varphi(r_0)}\sqrt{\frac{\pi}{2N\varphi''(r_0)}}\text{erfc}\left(\sqrt{\frac{N\varphi(r_o)''}{2}}(\sqrt{x}-r)\right), \tag{B-8}$$

where $r_0 = \sqrt{x}$ and $N \to \infty$. Now, we compute the integral of $\Gamma(Nx)$, whose derivation is similar to the integral given in eq. (B-7) with the difference $r \to \infty$. Then, we have

$$\Gamma(Nx) \sim 4N^{Nx}g(r_o)e^{-N\varphi(r_0)}\sqrt{\frac{\pi}{2N\varphi''(r_0)}}. \tag{B-9}$$

(B-10)

Inserting the results found in eq. (B-8) and eq. (B-9) in the eq. (B-4), we obtain that the incomplete gamma function in the limit of large N has the following asymptotic approximation

$$\frac{\Gamma(Nx, Nr^2)}{\Gamma(xN)} \sim 1 - \frac{1}{2}\text{erfc}\left(\sqrt{\frac{N\varphi(r_o)''}{2}}(\sqrt{x} - r)\right) \sim 1 - \frac{1}{2}\text{erfc}\left(\sqrt{2N}(\sqrt{x} - r)\right), \tag{B-11}$$

where we used that $\varphi(r_o)'' = 4$. Now, for the case when $\sqrt{x} > r'$, the integral (B-6) is solved as it is shown below

$$\int_0^r g(r')e^{-N\varphi(r')}dr' = \int_0^\infty g(r')e^{-N\varphi(r')}dr' - \int_r^\infty g(r')e^{-N\varphi(r')}dr', \tag{B-12}$$

where for the left integral we use the result found in the equation (B-7) when $r \to \infty$, and for the right integral we do the following

$$\begin{aligned}\int_r^\infty g(r')e^{-N\varphi(r')}dr' &\sim g(r_o)e^{-N\varphi(r_0)}\sqrt{\frac{2}{N\varphi''(r_0)}}\int_{\sqrt{\frac{N\varphi(r_o)''}{2}}(r-\sqrt{x})}^\infty e^{-y^2}dy \\ &\sim g(r_o)e^{-N\varphi(r_0)}\sqrt{\frac{\pi}{2N\varphi''(r_0)}}\text{erfc}(\sqrt{\frac{N\varphi(r_o)''}{2}}(r - \sqrt{x})).\end{aligned} \tag{B-13}$$

With this result, the integral (B-12) can be approximated as

$$\begin{aligned}\int_0^r g(r')e^{-N\varphi(r')}dr' &\sim g(r_o)e^{-N\varphi(r_0)}\sqrt{\frac{2}{N\varphi''(r_0)}}(2 - \text{erfc}(\sqrt{2N}(r - \sqrt{x}))) \\ &\sim g(r_o)e^{-N\varphi(r_0)}\sqrt{\frac{2}{N\varphi''(r_0)}}\text{erfc}\left(\sqrt{2N}(\sqrt{x} - r)\right),\end{aligned} \tag{B-14}$$

where we use that $\text{erfc}(x) + \text{erfc}(-x) = 2$. Then, for the second case, we obtain that the incomplete gamma function for large N has the following behavior

$$\frac{\Gamma(Nx, Nr^2)}{\Gamma(Nx)} \sim 1 - \frac{1}{2}\text{erfc}\left(\sqrt{2N}(\sqrt{x} - r)\right). \tag{B-15}$$

Thus, we conclude that it does not matter if $\sqrt{x} \leq r$ or $\sqrt{x} \geq r$, the result is the same. Then, we obtain the following important asymptotic approximation of $M_{xN}(r)$ for large N

$$M_{xN}(r) \sim 1 - \frac{1}{2}\text{erfc}\left(\sqrt{2N}(\sqrt{x} - r)\right). \tag{B-16}$$

Finally, using $M_{xN}(r) = 1 - L_{xN}(r)$, we arrive to

$$L_{xN}(r) \sim \frac{1}{2}\text{erfc}\left(\sqrt{2N}(\sqrt{x} - r)\right), \tag{B-17}$$

which was used in the derivation of the mean and the variance of κ and the cumulant generating function in the intermediate deviation regime in the section 3.2.

B.3. Derivation of the mean and variance of κ

B.3.1. Expected value of κ in the Ginibre ensemble

The formula for the expected value of κ is

$$\langle\kappa\rangle \sim \int_0^1 dx L_{xN}(r). \tag{B-18}$$

To solve this integral, we insert the asymptotic behavior of $L_{xN}(r)$ given in the equation (B-17) into the above integral and proceed to do the variable change $x = r^2 + \frac{u}{\sqrt{N}}$, which leads us to that $\sqrt{x} - r \approx \frac{u}{2r\sqrt{N}}$. Thus, we have that

$$\int_0^1 dx L_{xN}(r) \sim \frac{1}{\sqrt{N}} \int_{-r^2\sqrt{N}}^{(1-r^2)\sqrt{N}} du \frac{1}{2}\mathrm{erfc}\left(\frac{u}{\sqrt{2}r}\right),$$

which is solved using the formula $\int \mathrm{erfc}(ax)dx = x\mathrm{erfc}(ax) - \frac{1}{a\sqrt{\pi}}\exp(-a^2x^2)$ with $a = \frac{1}{\sqrt{2}r}$ (the formula can be found in [41]). The latter leads us to the following result

$$\frac{1}{\sqrt{N}} \int_{-r^2\sqrt{N}}^{(1-r^2)\sqrt{N}} du \frac{1}{2}\mathrm{erfc}\left(\frac{u}{\sqrt{2}r}\right) \sim \frac{r^2\sqrt{N}}{\sqrt{N}} \sim r^2.$$

Thus, the expected value of κ in the Ginibre ensemble for large N becomes

$$\langle\kappa\rangle \sim \int_0^1 dx L_{xN}(r) \sim r^2. \tag{B-19}$$

B.3.2. Variance of κ in the Ginibre ensemble

To compute the variance of κ, we use the corresponding formula given in (3-17) and proceed as follows

$$\mathrm{Var}(\kappa) \sim \frac{1}{N}\int_0^1 dx L_{xN}(r)(1 - L_{xN}(r)) \sim \frac{1}{N}\int_0^1 dx L_{xN}(r) M_{xN}(r), \tag{B-20}$$

where we use again the formula (B-17), which allows us to write the variance explicitly as

$$\mathrm{Var}(\kappa) \sim \frac{1}{4N}\int_0^1 dx \mathrm{erfc}(\sqrt{2N}(\sqrt{x} - r))\mathrm{erfc}(-\sqrt{2N}(\sqrt{x} - r)).$$

Then, we do the variable change $x = r^2 + \sqrt{\frac{2}{N}}ru$ which leads us to $u \approx \sqrt{2N}(\sqrt{x} - r)$. Thus, the integral for the variance is written now as

$$\mathrm{Var}(\kappa) \sim \frac{1}{4N}\sqrt{\frac{2}{N}}r \int_{-r\sqrt{\frac{N}{2}}}^{\sqrt{\frac{N}{2}}(1-r^2)/r} du \mathrm{erfc}(u)\mathrm{erfc}(-u),$$

where for large N this integral becomes in the following improper convergent integral

$$\mathrm{Var}(\kappa) \sim \frac{1}{4N}\sqrt{\frac{2}{N}}r \int_{-\infty}^{\infty} du \mathrm{erfc}(u)\mathrm{erfc}(-u) \sim 2\frac{1}{4N}\sqrt{\frac{2}{N}}r \int_0^{\infty} du \mathrm{erfc}(u)\mathrm{erfc}(-u).$$

Now, using the formula $\int_0^\infty du \mathrm{erfc}(u)\mathrm{erfc}(-u) = \sqrt{\frac{2}{\pi}}$, we arrive to

$$\mathrm{Var}(\kappa) \sim \frac{r}{\sqrt{\pi} N^{3/2}},$$

which corresponds to the result found in the equation (3-18) in the section 3.2.1 of the typical fluctuations of N_r.

C. Intermediate deviation regime

To solve this puzzle, we use the probability $\mathcal{P}_r(\kappa, N)$ in the large N limit given in the eq. (3-11), where we take $L_{xN}(r)$ as it is shown in the equation (3-20). With these ingredients, we write the PDF of κ as

$$\begin{aligned}\mathcal{P}_r(\kappa, N) &= \int_{\mathcal{C}} \frac{d\mu}{2\pi i} \exp\left[(\kappa - r^2)\mu N + N\int_0^{r^2} dx \log\left(1 + \frac{1}{2}\left(e^{\mu} - 1\right)\text{erfc}\left[\sqrt{2N}(\sqrt{x} - r)\right]\right)\right. \\ &\left. + N\int_{r^2}^{1} dx \log\left(1 + \frac{1}{2}\left(e^{-\mu} - 1\right)\text{erfc}\left[\sqrt{2N}(\sqrt{x} - r)\right]\right)\right. . \end{aligned} \tag{C-1}$$

Now, we do the variable change $x = r^2 + \sqrt{\frac{2}{N}}u$, which lead us to $\sqrt{x} - r \approx \frac{u}{\sqrt{2N}r}$ in the limit of large N. This change and algebraic manipulation, leads us to that the integral (C-1) can be expressed in terms of an inverse Laplace integral as in the eq. (3-21).

C.1. Asymptotic behaviour of the scaling function $\chi(\mu)$ for small μ

To compute the asymptotic behavior of the scaling function $\chi(\mu)$ given in the expression (3-22) when $\mu \to 0$, we focus on the integrand of the eq. (3-22), which we call $m(\mu, u)$, as follows

$$\begin{aligned} m(\mu, u) &= \log\left[1 + \sinh^2\left(\frac{\mu}{2}\right)\text{erfc}(u)\text{erfc}(-u)\right] \\ &\sim \frac{\mu^2}{4}\text{erfc}(u)\text{erfc}(-u) \quad \text{as} \quad \mu \to 0. \end{aligned} \tag{C-2}$$

With this asymptotic result, the integral (3-22) can be solved using that $\int_0^{\infty} du \text{erfc}(u)\text{erfc}(-u) = \sqrt{\frac{2}{\pi}}$ [41]. Thus, we obtain that $\chi(\mu)$ when $\mu \to 0$ is

$$\chi(\mu) \sim \frac{\mu^2}{4}\int_0^{\infty} du \text{erfc}(u)\text{erfc}(-u) \sim \frac{\mu^2}{2\sqrt{2\pi}}, \tag{C-3}$$

where this result is found in the first line of the equation (3-24)

C.2. Asymptotic behaviour of the scaling function $\chi(\mu)$ for large $|\mu|$

To compute the behavior of $\chi(\mu)$ given in the equation (3-22) in the limit of large $|\mu|$, we use as a guide a result found in [42]. To do this, we split the integral (3-22) as follows

$$\chi(\mu) = \int_0^{\sqrt{|\mu|}} du \log\left[1 + \sinh^2\left(\frac{\mu}{2}\right)\text{erfc}(u)\text{erfc}(-u)\right] + \int_{\sqrt{|\mu|}}^{\infty} du \log\left[1 + \sinh^2\left(\frac{\mu}{2}\right)\text{erfc}(u)\text{erfc}(-u)\right], \tag{C-4}$$

which lead us to that the second term in the above integral vanish . To check that the integral for $u > \sqrt{|\mu|}$ is zero, we use the asymptotic behavior of the following functions

$$\sinh^2(x) \sim \frac{e^{2|x|}}{4}, \quad x \to \pm\infty, \qquad \operatorname{erfc}(x)\operatorname{erfc}(-x) \sim 2\frac{e^{-x^2}}{\sqrt{\pi}x}, \quad x \to \infty. \tag{C-5}$$

Then, for $\mu \to \pm\infty$ and $u \to \infty$, the integrand term behaves as

$$m(\mu, u) = \log\left[1 + \sinh^2\left(\frac{\mu}{2}\right)\operatorname{erfc}(u)\operatorname{erfc}(-u)\right] \sim \log\left[1 + \frac{e^{|\mu|-u^2}}{2\sqrt{\pi}u}\right]. \tag{C-6}$$

Looking the term $|\mu| - u^2 = (\sqrt{|\mu|} - u)(\sqrt{|\mu|} + u)$, we can appreciate immediately that the above result vanish in the limit situation if $u > \sqrt{|\mu|}$. Then, only the left integral for large $|\mu|$ in the expression given in eq. (C-4) contributes to the solution, yielding us that the scaling function

$$\chi(\mu) \sim \int_0^{\sqrt{|\mu|}} du \log\left[1 + \frac{e^{|\mu|-u^2}}{2\sqrt{\pi}u}\right] \sim \int_0^{\sqrt{|\mu|}} du \log\left[\frac{e^{|\mu|-u^2}}{2\sqrt{\pi}u}\right] \sim \frac{2}{3}|\mu|^{3/2}, \quad \mu \to \pm\infty. \tag{C-7}$$

The above expression is found in the second line of the eqs. (3-24).

D. Saddle point equation for the atypical regime

In this appendix section we solve the saddle point equation which is found in the fourth line in the eqs. (3-31). Firstly, we split this integral as

$$\kappa = \int_0^{r^2} dx \frac{\mathrm{e}^{N\lambda^*} L_{xN}(r)}{\mathrm{e}^{N\lambda^*} L_{xN}(r) + M_{xN}(r)} + \int_{r^2}^1 dx \frac{\mathrm{e}^{N\lambda^*} L_{xN}(r)}{\mathrm{e}^{N\lambda^*} L_{xN}(r) + M_{xN}(r)}. \tag{D-1}$$

Then, we insert the uniform asymptotic expressions of $L_{xN}(r)$ and $M_{xN}(r)$ given in the eqs. (3-30). For $\lambda^* > 0$ we have for the left integral

$$\int_0^{r^2} \frac{\mathrm{e}^{N\lambda^*}(1 - \mathrm{e}^{N\varphi_r(x)})}{\mathrm{e}^{N\lambda^*}(1 - \mathrm{e}^{N\varphi_r(x)}) + \mathrm{e}^{-N\varphi_r(x)}} dx \sim \int_0^{r^2} dx \sim r^2, \tag{D-2}$$

where we use that $\varphi_r(x) = r^2 - x - x \log \frac{r^2}{x}$ is a positive convex function. For the right integral we have that it contributes only if $\lambda^* - \varphi_r(x) \geq 0$. Thus, we have

$$\int_{r^2}^1 \frac{\mathrm{e}^{N(\lambda^* - \varphi_r(x))}}{\mathrm{e}^{N(\lambda^* - \varphi_r(x))} + 1 - \mathrm{e}^{-N\varphi_r(x)}} dx \sim \int_{r^2}^{\min\{1, F(\lambda^*, r)\}} \frac{1}{1 + e^{-N(\lambda^* - \varphi_r(x))}} \sim \min\{1, F(\lambda^*, r)\} - r^2, \tag{D-3}$$

where $F(\lambda^*, r)$ is the solution in x of the equation $\lambda^* - \varphi_r(x) = 0$ for $r^2 \leq x \leq 1$. Thus, the saddle point λ^* is such that $\kappa = \min\{1, F(\lambda^*, r)\}$. With this result, the upper integration limit given in the right of the integral (3-34) is rewritten as κ. For the left tail we do a similar analisys ($\lambda^* < 0$). In this case, we have that only the left integral of the eq. (D-1) contributes to the the solution, as it is shown below

$$\int_0^{r^2} dx \frac{\mathrm{e}^{N\lambda^*} L_{xN}(r)}{\mathrm{e}^{N\lambda^*} L_{xN}(r) + M_{xN}(r)} \sim \int_0^{\max\{0, G(\lambda^*, r)\}} dx \frac{1}{1 + e^{-N(\lambda^* + \varphi_r(x))}} \sim \max\{0, G(\lambda^*, r)\}, \tag{D-4}$$

where $G(\lambda^*, r)$ is the solution in x of the equation $\lambda^* + \varphi_r(x) = 0$ for $0 < x \leq r^2$. Finally, the saddle point λ^* is such that $\kappa = \max\{0, G(\lambda^*, r)\}$.

Bibliography

[1] Satya N. Majumdar and Gregory Schehr. Large deviations. *arXiv e-prints*, page arXiv:1711.07571, Nov 2017.

[2] Pierpaolo Vivo. Large deviations of the maximum of independent and identically distributed random variables. *European Journal of Physics*, 36(5):1–14, 2015.

[3] Hugo Touchette. The large deviation approach to statistical mechanics. *Physics Reports*, 478(1-3):1–69, 2009.

[4] Angelo Vulpiani, Fabio Cecconi, Massimo Cencini, Andrea Puglisi, and Davide Vergni. Large deviations in physics. *The Legacy of the Law of Large Numbers (Berlin: Springer)*, 2014.

[5] Christopher Sebastian Hidalgo. Universal behavior of the full particle statistics of one-dimensional Coulomb gases with an arbitrary external potential, 2018.

[6] Liliana Blanco Castañeda. *Probabilidad*. Univ. Nacional de Colombia, 2004.

[7] Richard S Ellis. Large deviations for a general class of random vectors. *The Annals of Probability*, 12(1):1–12, 1984.

[8] Richard S Ellis. An overview of the theory of large deviations and applications to statistical mechanics. *Scandinavian Actuarial Journal*, 1995(1):97–142, 1995.

[9] Richard S Ellis. The theory of large deviations: from boltzmann's 1877 calculation to equilibrium macrostates in 2d turbulence. *Physica D: Nonlinear Phenomena*, 133(1-4):106–136, 1999.

[10] Richard S Ellis. The theory of large deviations and applications to statistical mechanics. In *lectures for international seminar on extreme events in complex dynamics*, 2006.

[11] Milton Abramowitz and Irene A Stegun. *Handbook of mathematical functions: with formulas, graphs, and mathematical tables*. Courier Corporation, 1965.

[12] Jinho Baik, Percy Deift, and Kurt Johansson. On the distribution of the length of the longest increasing subsequence of random permutations. *Journal of the American Mathematical Society*, 12(4):1119–1178, 1999.

[13] Michael Prähofer and Herbert Spohn. Universal distributions for growth processes in 1+ 1 dimensions and random matrices. *Physical review letters*, 84(21):4882–4885, 2000.

[14] Laurent Laloux, Pierre Cizeau, Marc Potters, and Jean-Philippe Bouchaud. Random matrix theory and financial correlations. *International Journal of Theoretical and Applied Finance*, 3(03):391–397, 2000.

[15] Giacomo Livan, Marcel Novaes, and Pierpaolo Vivo. *Introduction to Random Matrices: Theory and Practice*. Springer, 2018.

[16] Bertrand Lacroix-A-Chez-Toine, Aurélien Grabsch, Satya N Majumdar, and Grégory Schehr. Extremes of 2d coulomb gas: universal intermediate deviation regime. *Journal of Statistical Mechanics: Theory and Experiment*, 2018(1):013203, 2018.

[17] Madan Lal Mehta. *Random matrices*, volume 142. Elsevier, 2004.

[18] Ioana Dumitriu and Alan Edelman. Matrix models for beta ensembles. *Journal of Mathematical Physics*, 43(11):5830–5847, 2002.

[19] Satya N Majumdar and Grégory Schehr. Top eigenvalue of a random matrix: large deviations and third order phase transition. *Journal of Statistical Mechanics: Theory and Experiment*, 2014(1):01012, 2014.

[20] Manan Vyas and Thomas H Seligman. Random matrix ensembles for many-body quantum systems. In *AIP Conference Proceedings*, volume 1950. AIP Publishing, 2018.

[21] Myriam Charras-Garrido and Pascal Lezaud. Extreme value analysis: an introduction. *Journal de la Société Française de Statistique*, 154(2):66–97, 2013.

[22] Matteo Battilana. Order statistics of random walks, a test of universality. 2015.

[23] Craig A Tracy and Harold Widom. Level-spacing distributions and the airy kernel. *Communications in Mathematical Physics*, 159(1):151–174, 1994.

[24] Freeman J Dyson. Statistical theory of the energy levels of complex systems. i. *Journal of Mathematical Physics*, 3(1):140–156, 1962.

[25] Freeman J Dyson. Statistical theory of the energy levels of complex systems. ii. *Journal of Mathematical Physics*, 3(1):157–165, 1962.

[26] MM Fogler and BI Shklovskii. Probability of an eigenvalue number fluctuation in an interval of a random matrix spectrum. *Physical review letters*, 74(17):3312–3315, 1995.

[27] Ovidiu Costin and Joel L Lebowitz. Gaussian fluctuation in random matrices. *Physical Review Letters*, 75(1):69–72, 1995.

[28] Ricardo Marino, Satya N. Majumdar, Grégory Schehr, and Pierpaolo Vivo. Phase transitions and edge scaling of number variance in gaussian random matrices. *Phys. Rev. Lett.*, 112:254101, Jun 2014.

[29] Ricardo Marino, Satya N. Majumdar, Grégory Schehr, and Pierpaolo Vivo. Number statistics for β-ensembles of random matrices: Applications to trapped fermions at zero temperature. *Phys. Rev. E*, 94:032115, Sep 2016.

[30] Jean Ginibre. Statistical ensembles of complex, quaternion, and real matrices. *Journal of Mathematical Physics*, 6(3):440–449, 1965.

[31] V. Girko. Circular law. *Theory of Probability And Its Applications*, 29(4):694–706, 1985.

[32] Charles Bordenave and Djalil Chafaï. Around the circular law. *Probability surveys*, 9:1–89, 2012.

[33] Fabio Deelan Cunden, Francesco Mezzadri, and Pierpaolo Vivo. Large deviations of radial statistics in the two-dimensional one-component plasma. *Journal of Statistical Physics*, 164(5):1062–1081, 2016.

[34] Romain Allez, Jonathan Touboul, and Gilles Wainrib. Index distribution of the ginibre ensemble. *Journal of Physics A: Mathematical and Theoretical*, 47(4):042001, 2014.

[35] NM Temme. Uniform asymptotic expansions of the incomplete gamma functions and the incomplete beta function. *Mathematics of Computation*, 29(132):1109–1114, 1975.

[36] Bertrand Lacroix-A-Chez-Toine, Jeyson Andrés Monroy Garzón, Christopher Sebastian Hidalgo Calva, Isaac Pérez Castillo, Anupam Kundu, Satya N Majumdar, and Grégory Schehr. Intermediate deviation regime for the full eigenvalue statistics in the complex ginibre ensemble. *Physical Review E*, 100(1):012137, 2019.

[37] Alexander K Hartmann and Marc Mézard. Distribution of diameters for erdős-rényi random graphs. *Physical Review E*, 97(3):032128, 2018.

[38] Bertrand Lacroix-A-Chez-Toine, Satya N Majumdar, and Grégory Schehr. Rotating trapped fermions in two dimensions and the complex ginibre ensemble: Exact results for the entanglement entropy and number variance. *Physical Review A*, 99(2):021602, 2019.

[39] Rafael Díaz Hernández Rojas, Christopher Sebastian Hidalgo Calva, and Isaac Pérez Castillo. Universal behavior of the full particle statistics of one-dimensional coulomb gases with an arbitrary external potential. *Physical Review E*, 98(2):020104, 2018.

[40] George B Arfken and Hans J Weber. *Mathematical methods for physicists*. American Journal of Physics, 1999.

[41] Edward W Ng and Murray Geller. A table of integrals of the error functions. *Journal of Research of the National Bureau of Standards B*, 73(1):1–20, 1969.

[42] Paul L Krapivsky, Kirone Mallick, and Tridib Sadhu. Tagged particle in single-file diffusion. *Journal of Statistical Physics*, 160(4):885–925, 2015.